

Muon (g-2) and thermal WIMP DM in $U(1)_{L_\mu - L_\tau}$ Models

Pyungwon Ko (KIAS)

Scalars2023, U of Warsaw
Sep 13-16 (2023)

$U(1)_{L_\mu - L_\tau}$ -charged DM

: Z' only vs. $Z' + \phi$

Based on arXiv: 2204.04889
With Seungwon Baek, Jongkuk Kim

cf: Let me call Z' , $U(1)_{L_\mu - L_\tau}$ gauge boson,
“dark photon”, since it couples to DM

Contents

- Why dark Higgs ?
- $U(1)_{L_\mu - L_\tau}$ Models : Muon g-2, leptophilic fermion DM and PAMELA e^+ excess, etc.
- More on scalar/fermion DM w/o and w/ dark Higgs ϕ
- Conclusions

Why Dark Higgs ?

Dark Gauge Symmetry

Z_2 real scalar DM

- Simplest DM model with Z_2 symmetry : $S \rightarrow -S$

$$\mathcal{L} = \frac{1}{2}\partial_\mu S\partial^\mu S - \frac{1}{2}m_S^2 S^2 - \frac{\lambda_S}{4!}S^4 - \frac{\lambda_{SH}}{2}S^2 H^\dagger H.$$
- Global Z_2 could be broken by gravity effects (higher dim operators)
- e.g. consider Z_2 breaking dim-5 op : $\frac{1}{M_{\text{Planck}}} SO_{\text{SM}}^{(4)}$
- Lifetime of EW scale mass “S” is too short to be a DM
- Similarly for singlet fermion DM

Fate of CDM with Z_2 sym

(Baek,Ko,Park,arXiv:1303.4280)

Consider Z_2 breaking operators such as

$$\frac{1}{M_{\text{Planck}}} \overset{3}{SO}_{\text{SM}} \overset{3}{}$$

keeping dim-4 SM
operators only

The lifetime of the Z_2 symmetric scalar CDM S is roughly given by

$$\Gamma(S) \sim \frac{m_S}{M_{\text{Planck}}^2} \sim \left(\frac{m_S}{100 \text{GeV}} \right) 10^{-37} \text{GeV}$$

- Global Z_2 cannot save EW scale DM from decay with long enough lifetime

The lifetime is too short for ~ 100 GeV DM

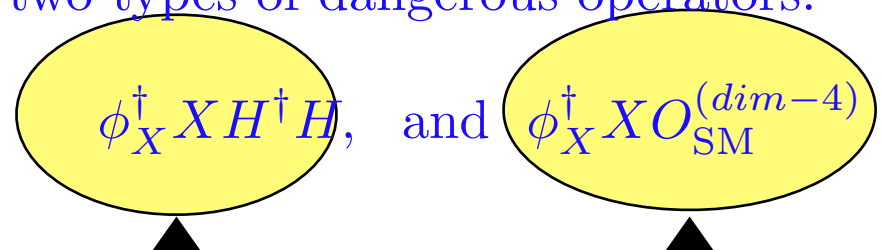
Fate of CDM with Z_2 sym

Spontaneously broken local $U(1)_X$ can do the job to some extent, but there is still a problem

Let us assume a local $U(1)_X$ is spontaneously broken by $\langle \phi_X \rangle \neq 0$ with

$$Q_X(\phi_X) = Q_X(X) = 1$$

Then, there are two types of dangerous operators:



Problematic !

Perfectly fine !

- **Higgs is not good for DM stability/longevity**
- **This is true for sermonic DM too**

$$Q_X(\phi) = 2, \quad Q_X(X) = 1$$

arXiv:1407.6588 w/ WIPark and SBaek

$$\begin{aligned}\mathcal{L} = & \mathcal{L}_{\text{SM}} + -\frac{1}{4}X_{\mu\nu}X^{\mu\nu} - \frac{1}{2}\epsilon X_{\mu\nu}B^{\mu\nu} + D_\mu\phi_X^\dagger D^\mu\phi_X - \frac{\lambda_X}{4}\left(\phi_X^\dagger\phi_X - v_\phi^2\right)^2 + D_\mu X^\dagger D^\mu X - m_X^2 X^\dagger X \\ & - \frac{\lambda_X}{4}(X^\dagger X)^2 - (\mu X^2\phi^\dagger + H.c.) - \frac{\lambda_{XH}}{4}X^\dagger X H^\dagger H - \frac{\lambda_{\phi_X H}}{4}\phi_X^\dagger\phi_X H^\dagger H - \frac{\lambda_{XH}}{4}X^\dagger X\phi_X^\dagger\phi_X\end{aligned}$$

The lagrangian is invariant under $X \rightarrow -X$ even after $U(1)_X$ symmetry breaking.

Unbroken Local Z₂ symmetry Gauge models for excited DM

$X_R \rightarrow X_I \gamma_h^*$ followed by $\gamma_h^* \rightarrow \gamma \rightarrow e^+e^-$ etc.

The heavier state decays into the lighter state

- The local Z₂ model is not that simple as the usual Z₂ scalar DM model (also for the fermion CDM)
- DM phenomenology richer and DM stability/longevity on much solider ground

Local dark gauge symmetry

- Better to use local gauge symmetry for DM stability in the presence of gravity [Beek,Ko,Park,arXiv:1303.4280]

- Success of the Standard Model of Particle Physics lies in “local gauge symmetry” without imposing any internal global symmetries
- Electron stability : $U(1)_{\text{em}}$ gauge invariance, electric charge conservation, massless photon
- Proton longevity : baryon # is an accidental sym of the SM
- No gauge singlets in the SM ; all the SM fermions chiral

- Dark sector with (excited) dark matter, dark radiation and force mediators might have the same structure as the SM
- “(Chiral) dark gauge theories without any global sym”
- Origin of DM stability/longevity from dark gauge sym, and not from dark global symmetries, as in the SM
- Just like the SM (conservative)

Singlet Portals to DM

[Beek,Ko,Park,arXiv:1303.4280]

- Higgs portal : $H^\dagger HS, H^\dagger HS^2, H^\dagger H\phi^\dagger\phi$ ϕ : Dark Scalars
- U(1) Vector portal : $\epsilon B_{\mu\nu} X^{\mu\nu}$ X_μ : Dark photon
- Neutrino portal : $\overline{N}_R (\widetilde{H} l_L + \phi^\dagger \psi)$ ψ : Dark fermion
~ Sterile ν
- So on & on & on ...
- Eventually “Portal” is what we observe in the experiments

In QFT,

- DM could be absolutely stable due to unbroken local gauge symmetry (DM with local Z_2 , Z_3 etc.) or topology (hidden sector monopole + vector DM + dark radiation)
- Longevity of DM due to some accidental symmetries (Strongly interacting hidden sector (DQCD), dark pions and dark baryons : Ko et al (2007,2011))
- Kinematically long-lived if DM is very light (axion, sterile ν_s , etc..)

Dark Higgs Important

- Since the symmetry breaking patterns of dark gauge symmetry are determined by dark Higgs charges (or their representations)
- $U(1) \rightarrow 0$ or Z_2 or Z_3 , etc. [inelastic DM (2014), semi-annihilation (2013), SIDM, etc.]
- $SO(3) \rightarrow SO(2)$: hidden monopole DM, VDM, DR [Baek, PK, Park (2013)]
- $SU(3) \rightarrow SU(2)$: $\Delta N_{\text{eff}}, H_0 \cdot \sigma_8$ [PK, Yong Tang (2016)]

Z_2 DM models with dark Higgs

- We solve this inconsistency and unitarity issue with Krauss-Wilczek mechanism
- By introducing a dark Higgs, we have many advantages:
 - Dark photon gets massive
 - Mass gap δ is generated by dark Higgs mechanism
 - We can have DM pair annihilation in P-wave involving dark Higgs in the final states, unlike in other works

Usual Approaches

For example, Harigaya, Nagai, Suzuki, arXiv:2006.11938

$$V(\phi) = m^2|\phi|^2 + \Delta^2 (\phi^2 + \phi^{*2}), \quad (1)$$

This term is problematic

$$\mathcal{L} = g_D A'^\mu (\chi_1 \partial_\mu \chi_2 - \chi_2 \partial_\mu \chi_1) + \epsilon e A'_\mu J_{EM}^\mu,$$

Similarly for the fermion DM case

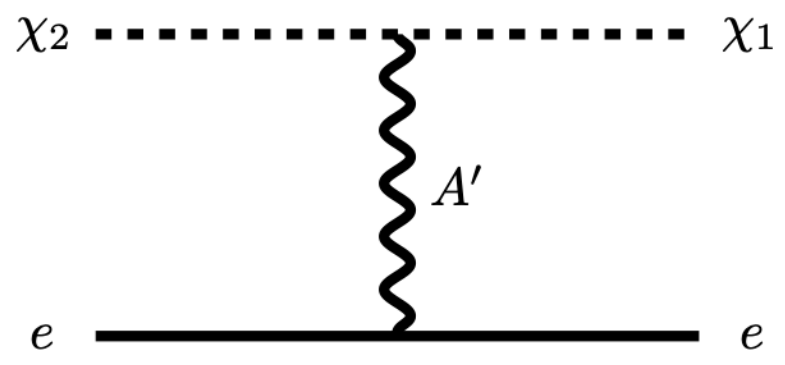


FIG. 1. Inelastic scattering of the heavier DM particle χ_2 off the electron e into the lighter particle χ_1 , mediated by the dark photon A' .

- The model is not mathematically consistent, since there is no conserved current a dark photon can couple to in the massless limit
- The second term with Δ^2 breaks $U(1)_X$ explicitly, although softly

Relic Density from

$$XX^\dagger \rightarrow Z'{}^* \rightarrow f\bar{f}$$

(P-wave annihilation)

For example, Harigaya, Nagai, Suzuki, arXiv:2006.11938

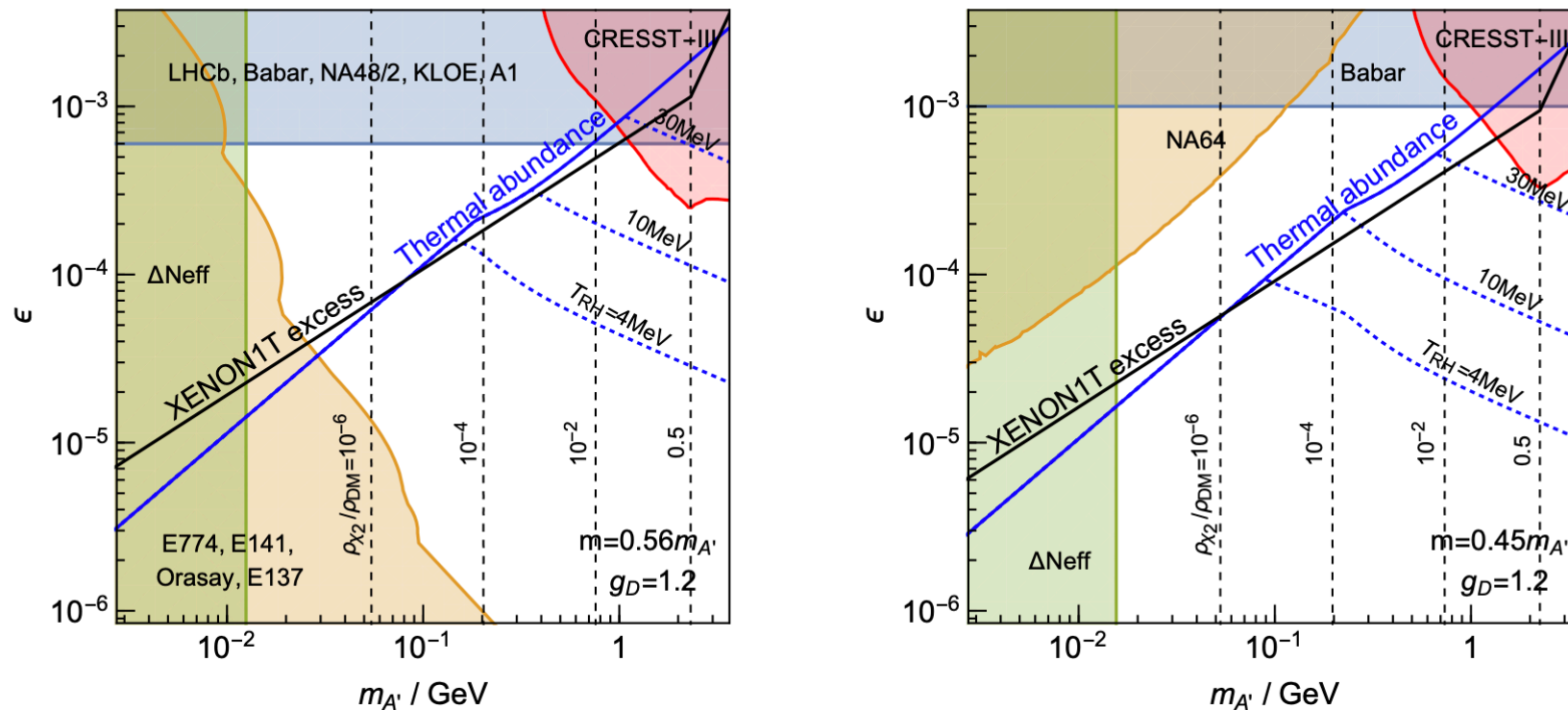


FIG. 4. The required value of ϵ to explain the observed excess of events at XENON1T in terms of the dark photon mass $m_{A'}$ (black solid lines). The left and right panels correspond to the cases of $m > m_{A'}/2$ and $m < m_{A'}/2$ respectively. We assume $g_D = 1.2$ in both cases. The blue lines denote the required value of ϵ to obtain the observed DM abundance by the thermal freeze-out process, discussed in Sec. IV. The solid lines correspond to the case without any entropy production. The dashed lines assume freeze-out during a matter dominated era and the subsequent reheating at T_{RH} , which suppresses the DM abundance by a factor of $(T_{\text{RH}}/T_{\text{FO}})^3$. The black dashed lines denote the mass density of χ_2 normalized by the total DM density. The shaded regions show the constraints from dark radiation and various searches for the dark photon A' which are discussed in Sec. V.

Scalar XDM (X_R & X_I)

Field	ϕ	X	χ
U(1) charge	2	1	1

$$\begin{aligned} \mathcal{L} = & \mathcal{L}_{\text{SM}} - \frac{1}{4} \hat{X}_{\mu\nu} \hat{X}^{\mu\nu} - \frac{1}{2} \sin \epsilon \hat{X}_{\mu\nu} \hat{B}^{\mu\nu} + D^\mu \phi^\dagger D_\mu \phi + D^\mu X^\dagger D_\mu X - m_X^2 X^\dagger X + m_\phi^2 \phi^\dagger \phi \\ & - \lambda_\phi (\phi^\dagger \phi)^2 - \lambda_X (X^\dagger X)^2 - \lambda_{\phi X} X^\dagger X \phi^\dagger \phi - \lambda_{\phi H} \phi^\dagger \phi H^\dagger H - \lambda_{H X} X^\dagger X H^\dagger H \\ & - \mu (X^2 \phi^\dagger + H.c.) , \end{aligned} \quad (1)$$

$$X = \frac{1}{\sqrt{2}}(X_R + iX_I),$$

$$\mathcal{L} \supset \epsilon g_X s_W Z^\mu (X_R \partial_\mu X_I - X_I \partial_\mu X_R) - \frac{g_Z}{2} Z_\mu \bar{\nu}_L \gamma^\mu \nu_L.$$

$$H = \begin{pmatrix} 0 \\ \frac{1}{\sqrt{2}}(v_H + h_H) \end{pmatrix}, \quad \phi = \frac{1}{\sqrt{2}}(v_\phi + h_\phi),$$

$$\mathcal{L} \supset g_X Z'^\mu (X_R \partial_\mu X_I - X_I \partial_\mu X_R) - \epsilon e c_W Z'_\mu \bar{e} \gamma^\mu e,$$

$$U(1) \rightarrow Z_2 \text{ by } v_\phi \neq 0 : X \rightarrow -X$$

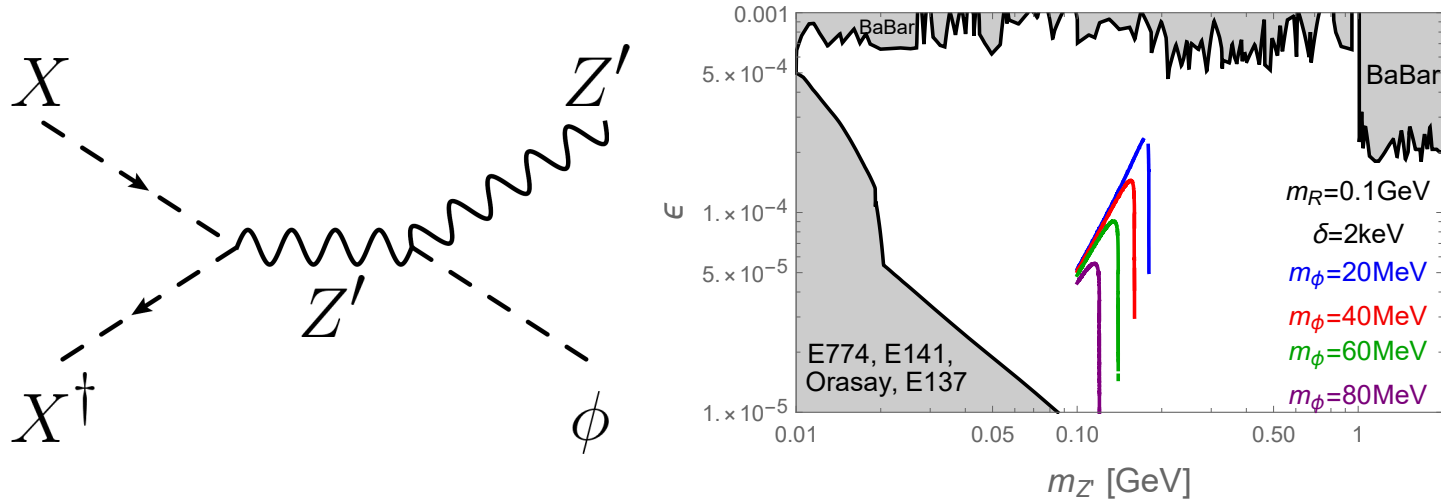


FIG. 1: (*left*) Feynman diagrams relevant for thermal relic density of DM: $XX^\dagger \rightarrow Z'\phi$ and (*right*) the region in the $(m_{Z'}, \epsilon)$ plane that is allowed for the XENON1T electron recoil excess and the correct thermal relic density for scalar DM case for $\delta = 2$ keV : (a) $m_{\text{DM}} = 0.1$ GeV. Different colors represents $m_\phi = 20, 40, 60, 80$ MeV. The gray areas are excluded by various experiments, from BaBar [61], E774 [62], E141 [63], Orasay [64], and E137 [65], assuming $Z' \rightarrow X_R X_I$ is kinematically forbidden.

P-wave annihilation x-sections

Scalar DM : $XX^\dagger \rightarrow Z'^* \rightarrow Z'\phi$

$$\begin{aligned} \sigma v &\simeq \frac{g_X^4 v^2}{384\pi m_X^4 (4m_X^2 - m_{Z'}^2)^2} (16m_X^4 + m_{Z'}^4 + m_\phi^4 + 40m_X^2 m_{Z'}^2 - 8m_X^2 m_\phi^2 - 2m_{Z'}^2 m_\phi^2) \\ &\times \left[\{4m_X^2 - (m_{Z'} + m_\phi)^2\} \{4m_X^2 - (m_{Z'} - m_\phi)^2\} \right]^{1/2} + \mathcal{O}(v^4), \end{aligned} \quad (10)$$

Fermion XDM (χ_R & χ_I)

$$\begin{aligned}\mathcal{L} = & -\frac{1}{4}\hat{X}^{\mu\nu}\hat{X}_{\mu\nu} - \frac{1}{2}\sin\epsilon\hat{X}_{\mu\nu}B^{\mu\nu} + \bar{\chi}(i\cancel{D} - m_\chi)\chi + D_\mu\phi^\dagger D^\mu\phi \\ & - \mu^2\phi^\dagger\phi - \lambda_\phi|\phi|^4 - \frac{1}{\sqrt{2}}\left(y\phi^\dagger\overline{\chi^C}\chi + \text{h.c.}\right) - \lambda_{\phi H}\phi^\dagger\phi H^\dagger H\end{aligned}$$

$$\begin{aligned}\chi &= \frac{1}{\sqrt{2}}(\chi_R + i\chi_I), \\ \chi^c &= \frac{1}{\sqrt{2}}(\chi_R - i\chi_I), \\ \chi_R^c &= \chi_R, \quad \chi_I^c = \chi_I,\end{aligned}$$

$$\begin{aligned}\mathcal{L} = & \frac{1}{2}\sum_{i=R,I}\bar{\chi}_i(i\cancel{D} - m_i)\chi_i - i\frac{g_X}{2}(Z'_\mu + \epsilon_{SW}Z_\mu)(\bar{\chi}_R\gamma^\mu\chi_I - \bar{\chi}_I\gamma^\mu\chi_R) \\ & - \frac{1}{2}yh_\phi(\bar{\chi}_R\chi_R - \bar{\chi}_I\chi_I),\end{aligned}$$

$U(1) \rightarrow Z_2$ by $v_\phi \neq 0 : \chi \rightarrow -\chi$

arXiv:2006.16876, PLB 810 (2020) 135848
 With Seungwon Baek, Jongkuk Kim

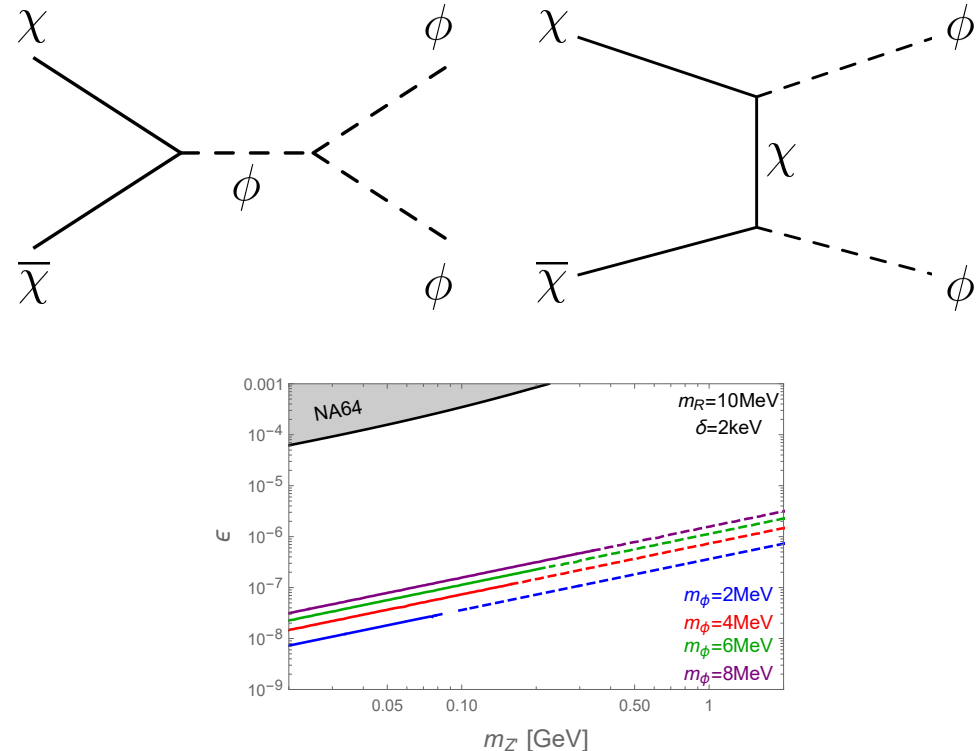


FIG. 2: (*top*) Feynman diagrams for $\chi\bar{\chi} \rightarrow \phi\phi$. (*bottom*) the region in the $(m_{Z'}, \epsilon)$ plane that is allowed for the XENON1T electron recoil excess and the correct thermal relic density for fermion DM case for $\delta = 2 \text{ keV}$ and the fermion DM mass to be $m_R = 10 \text{ MeV}$. Different colors represents $m_\phi = 2, 4, 6, 8 \text{ MeV}$. The gray areas are excluded by various experiments, assuming $Z' \rightarrow \chi_R \chi_I$ is kinematically allowed, and the experimental constraint is weaker in the ϵ we are interested in, compared with the scalar DM case in Fig. 1 (right). We also show the current experimental bounds by NA64 [66].

P-wave annihilation x-sections

Scalar DM : $XX^\dagger \rightarrow Z'^* \rightarrow Z'\phi$

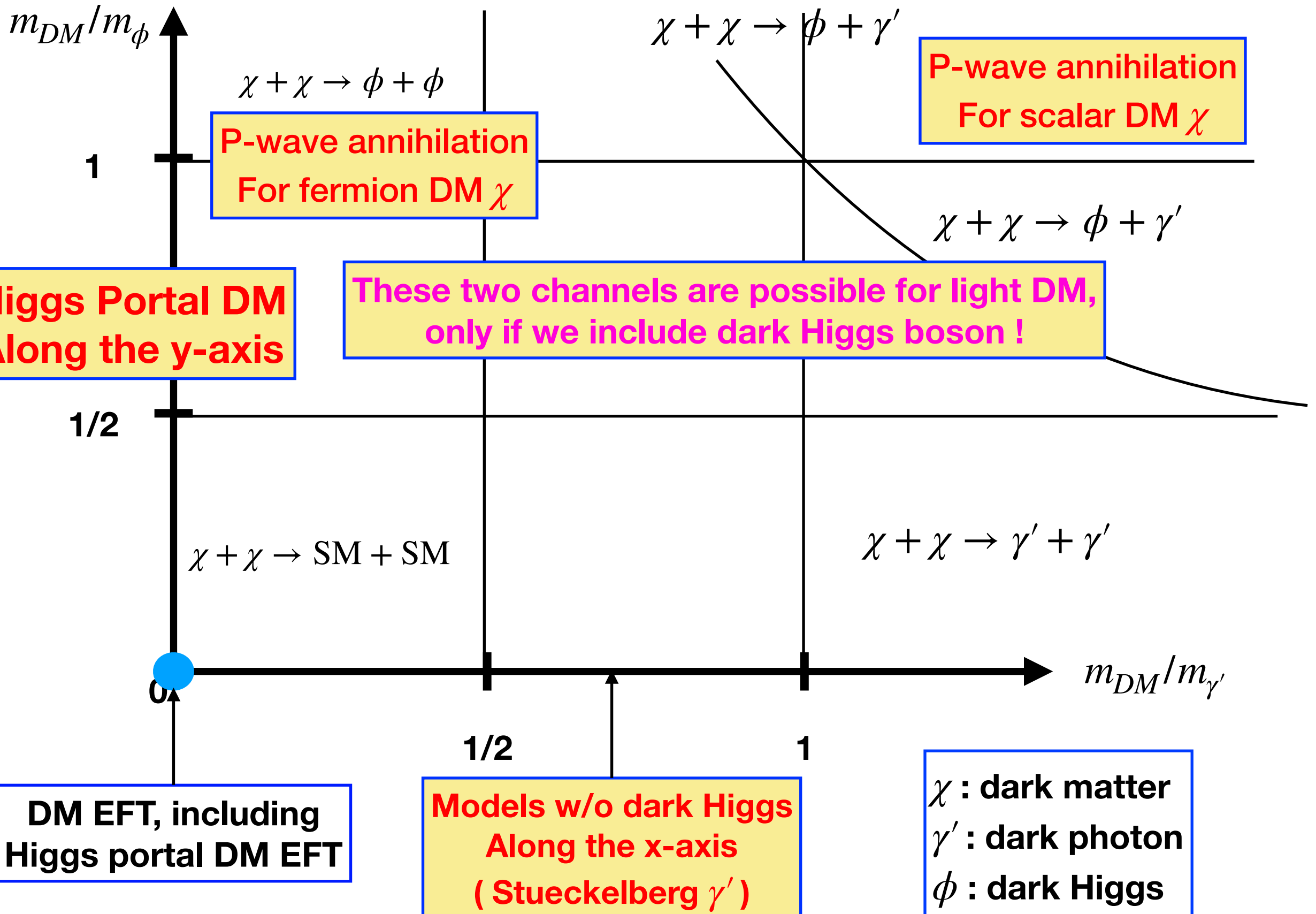
$$\begin{aligned} \sigma v &\simeq \frac{g_X^4 v^2}{384\pi m_X^4 (4m_X^2 - m_{Z'}^2)^2} (16m_X^4 + m_{Z'}^4 + m_\phi^4 + 40m_X^2 m_{Z'}^2 - 8m_X^2 m_\phi^2 - 2m_{Z'}^2 m_\phi^2) \\ &\times \left[\{4m_X^2 - (m_{Z'} + m_\phi)^2\} \{4m_X^2 - (m_{Z'} - m_\phi)^2\} \right]^{1/2} + \mathcal{O}(v^4), \end{aligned} \quad (10)$$

Fermion DM : $\chi\bar{\chi} \rightarrow \phi\phi$

$$\sigma v = \frac{y^2 v^2 \sqrt{m_\chi^2 - m_\phi^2}}{96\pi m_\chi} \left[\frac{27\lambda_\phi^2 v_\phi^2}{(4m_\chi^2 - m_\phi^2)^2} + \frac{4y^2 m_\chi^2 (9m_\chi^4 - 8m_\chi^2 m_\phi^2 + 2m_\phi^4)}{(2m_\chi^2 - m_\phi^2)^4} \right] + \mathcal{O}(v^4), \quad (28)$$

**Crucial to include “dark Higgs” to have
DM pair annihilation in P-wave**

Dark sector parameter space for a fixed m_{DM}



Higgs Portal DM : EFT vs. UV completions

$$\Gamma_{\text{inv}}(H \rightarrow VV) \text{ for } m_V \rightarrow 0$$

arXiv: 2112.11983, PRD 105 (2022) 015007, with S. Baek, W.I. Park
And references therein by P. Ko et al

Higgs portal DM models

$$\mathcal{L}_{\text{scalar}} = \frac{1}{2} \partial_\mu S \partial^\mu S - \frac{1}{2} m_S^2 S^2 - \frac{\lambda_{HS}}{2} H^\dagger H S^2 - \frac{\lambda_S}{4} S^4$$

$$\mathcal{L}_{\text{fermion}} = \overline{\psi} [i\gamma \cdot \partial - m_\psi] \psi - \frac{\lambda_{H\psi}}{\Lambda} H^\dagger H \overline{\psi} \psi$$

$$\mathcal{L}_{\text{vector}} = -\frac{1}{4} V_{\mu\nu} V^{\mu\nu} + \frac{1}{2} m_V^2 V_\mu V^\mu + \frac{1}{4} \lambda_V (V_\mu V^\mu)^2 + \frac{1}{2} \lambda_{HV} H^\dagger H V_\mu V^\mu.$$

All invariant
under ad hoc
 Z_2 symmetry

arXiv:1112.3299, ... 1402.6287, etc.

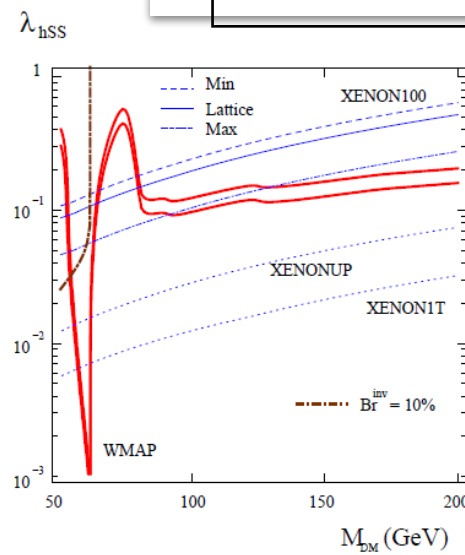


FIG. 1. Scalar Higgs-portal parameter space allowed by WMAP (between the solid red curves), XENON100 and $\text{Br}^{\text{inv}} = 10\%$ for $m_h = 125$ GeV. Shown also are the prospects for XENON upgrades.

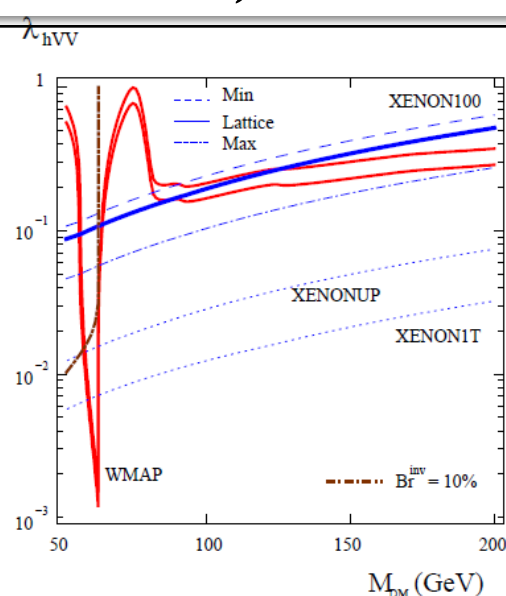


FIG. 2. Same as Fig. 1 for vector DM particles.

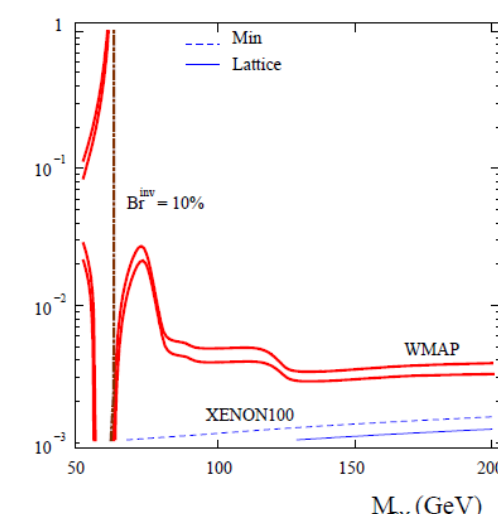


FIG. 3. Same as in Fig. 1 for fermion DM; λ_{hff}/Λ is in GeV^{-1} .

Higgs portal DM as examples

$$\mathcal{L}_{\text{scalar}} = \frac{1}{2} \partial_\mu S \partial^\mu S - \frac{1}{2} m_S^2 S^2 - \frac{\lambda_{HS}}{2} H^\dagger H S^2 - \frac{\lambda_S}{4} S^4$$

$$\mathcal{L}_{\text{fermion}} = \bar{\psi} [i\gamma \cdot \partial - m_\psi] \psi - \frac{\lambda_{H\psi}}{\Lambda} H^\dagger H \bar{\psi} \psi$$

$$\mathcal{L}_{\text{vector}} = -\frac{1}{4} V_{\mu\nu} V^{\mu\nu} + \frac{1}{2} m_V^2 V_\mu V^\mu + \frac{1}{4} \lambda_V (V_\mu V^\mu)^2 + \frac{1}{2} \lambda_{HV} H^\dagger H V_\mu V^\mu.$$

All invariant
under ad hoc
 Z_2 symmetry

arXiv:1112.3299, ... 1402.6287, etc.

And Revived recent papers

We need to include dark Higgs or singlet scalar
to get renormalizable/unitary models
for Higgs portal singlet fermion or vector DM
[NB: UV Completions : Not unique]

$m_h = 125$ GeV. Shown also are the prospects for XENON upgrades.

FIG. 2. Same as Fig. 1 for vector DM particles.

FIG. 3. Same as in Fig.1 for fermion DM; λ_{hff}/Λ is in GeV

Models for HP SFDM & VDM

UV Completion of HP Singlet Fermion DM (SFDM)

$$\begin{aligned}\mathcal{L} = & \mathcal{L}_{\text{SM}} - \mu_{HS} S H^\dagger H - \frac{\lambda_{HS}}{2} S^2 H^\dagger H \\ & + \frac{1}{2} (\partial_\mu S \partial^\mu S - m_S^2 S^2) - \mu'_S S - \frac{\mu'_S}{3} S^3 - \frac{\lambda_S}{4} S^4 \\ & + \bar{\psi} (i \not{\partial} - m_{\psi_0}) \psi - \lambda S \bar{\psi} \psi\end{aligned}$$

UV Completion of HP VDM

$$\begin{aligned}\mathcal{L}_{VDM} = & -\frac{1}{4} X_{\mu\nu} X^{\mu\nu} + (D_\mu \Phi)^\dagger (D^\mu \Phi) - \frac{\lambda_\Phi}{4} \left(\Phi^\dagger \Phi - \frac{v_\Phi^2}{2} \right)^2 \\ & - \lambda_{H\Phi} \left(H^\dagger H - \frac{v_H^2}{2} \right) \left(\Phi^\dagger \Phi - \frac{v_\Phi^2}{2} \right),\end{aligned}$$

- The simplest UV completions in terms of # of new d.o.f.
- At least, 2 more parameters, (m_ϕ , $\sin \alpha$) for DM physics

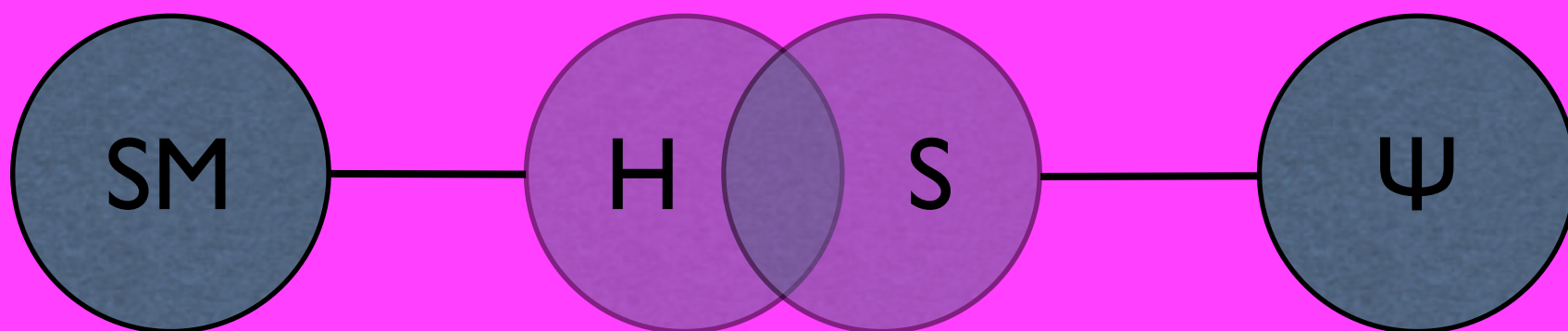
UV Completion for HP FDM

Baek, Ko, Park, arXiv:1112.1847

$$\begin{aligned}\mathcal{L} = \mathcal{L}_{\text{SM}} &+ \mu_{HS} S H^\dagger H - \frac{\lambda_{HS}}{2} S^2 H^\dagger H \\ &+ \frac{1}{2} (\partial_\mu S \partial^\mu S - m_S^2 S^2) - \mu_S^3 S - \frac{\mu'_S}{3} S^3 - \frac{\lambda_S}{4} S^4 \\ &+ \bar{\psi} (i \not{\partial} - m_{\psi_0}) \psi - \lambda S \bar{\psi} \psi\end{aligned}$$

mixing

invisible decay



Production and decay rates are suppressed relative to SM.

Higgs-Singlet Mixing

- Mixing and Eigenstates of Higgs-like bosons

$$\begin{aligned}\mu_H^2 &= \lambda_H v_H^2 + \mu_{HS} v_S + \frac{1}{2} \lambda_{HS} v_S^2, \\ m_S^2 &= -\frac{\mu_S^3}{v_S} - \mu'_S v_S - \lambda_S v_S^2 - \frac{\mu_{HS} v_H^2}{2v_S} - \frac{1}{2} \lambda_{HS} v_H^2,\end{aligned}$$

at vacuum

$$M_{\text{Higgs}}^2 \equiv \begin{pmatrix} m_{hh}^2 & m_{hs}^2 \\ m_{hs}^2 & m_{ss}^2 \end{pmatrix} \equiv \begin{pmatrix} \cos \alpha & \sin \alpha \\ -\sin \alpha & \cos \alpha \end{pmatrix} \begin{pmatrix} m_1^2 & 0 \\ 0 & m_2^2 \end{pmatrix} \begin{pmatrix} \cos \alpha & -\sin \alpha \\ \sin \alpha & \cos \alpha \end{pmatrix}$$

$$\begin{aligned}H_1 &= h \cos \alpha - s \sin \alpha, \\ H_2 &= h \sin \alpha + s \cos \alpha.\end{aligned}$$

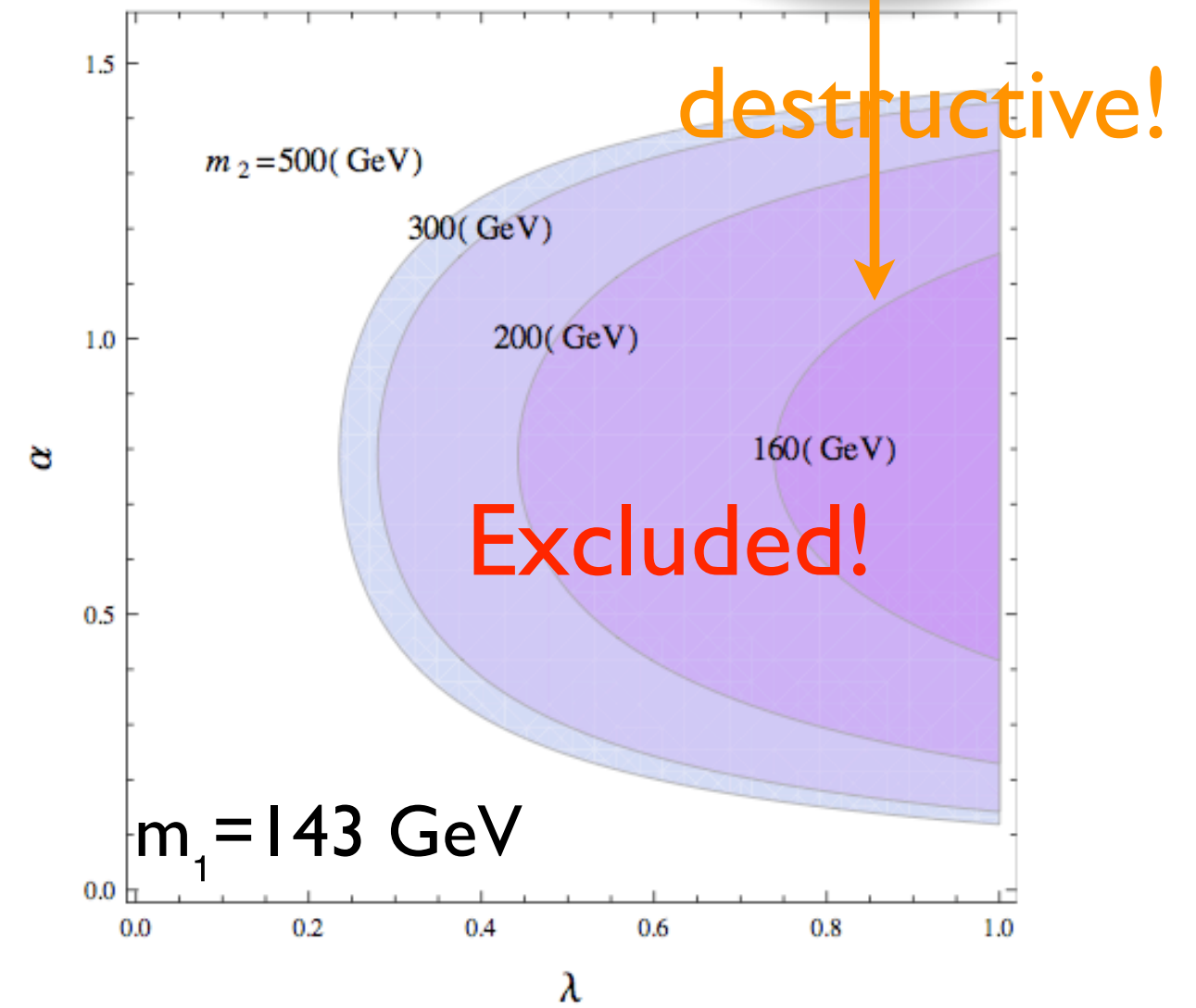
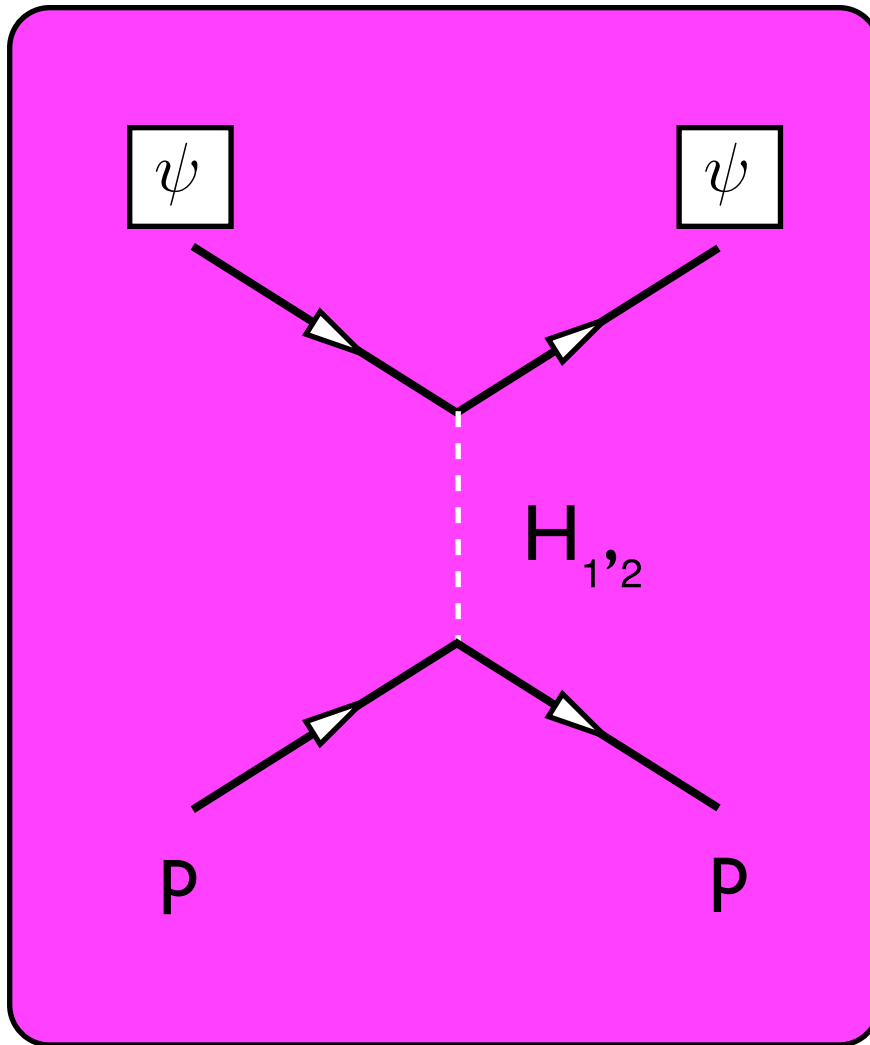


Mixing of Higgs and singlet

Constraints

- Dark matter to nucleon cross section (constraint)

$$\sigma_p \approx \frac{1}{\pi} \mu^2 \lambda_p^2 \simeq 2.7 \times 10^{-2} \frac{m_p^2}{\pi} \left| \left(\frac{m_p}{v} \right) \lambda \sin \alpha \cos \alpha \left(\frac{1}{m_1^2} - \frac{1}{m_2^2} \right) \right|^2$$

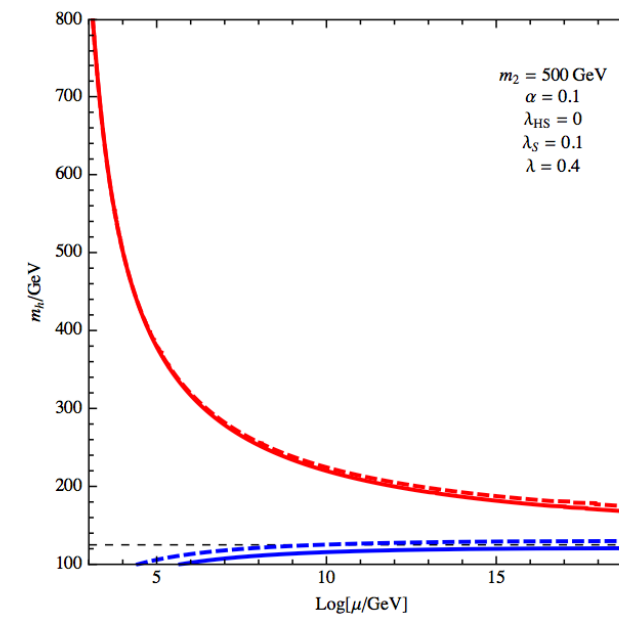
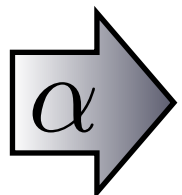
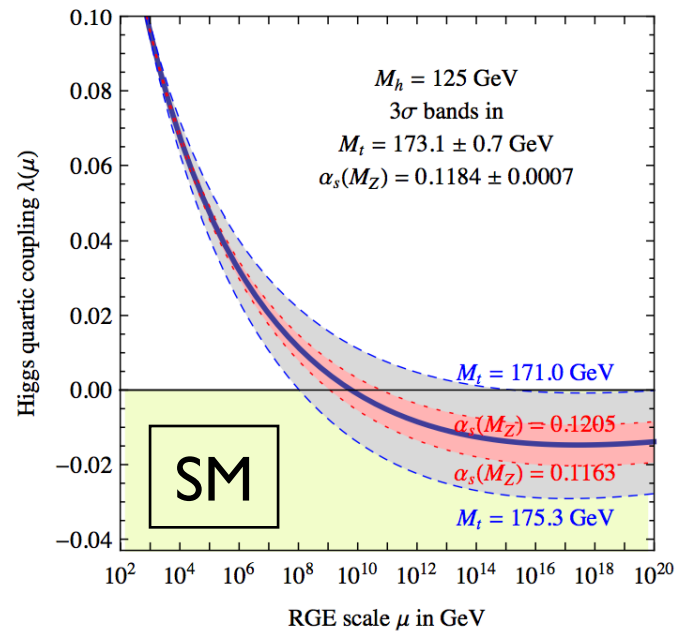


Low energy pheno.

- Universal suppression of collider SM signals
[See 1112.1847, Seungwon Baek, P.Ko & WIP]
- If “ $m_h > 2 m_\phi$ ”, non-SM Higgs decay!
- Tree-level shift of $\lambda_{H,\text{SM}}$ (& loop correction)

$$\lambda_{\Phi H} \Rightarrow \lambda_H = \left[1 + \left(\frac{m_\phi^2}{m_h^2} - 1 \right) \sin^2 \alpha \right] \lambda_H^{\text{SM}}$$

→ If “ $m_\phi > m_h$ ”, vacuum instability can be cured.



[G. Degrassi et al., 1205.6497]

[S. Baek, P. Ko, WIP & E. Senaha, JHEP(2012)]

UV Completion of HP VDM

[S Baek, P Ko, WI Park, E Senaha, arXiv:1212.2131 (JHEP)]

$$\mathcal{L}_{VDM} = -\frac{1}{4}X_{\mu\nu}X^{\mu\nu} + (D_\mu\Phi)^\dagger(D^\mu\Phi) - \frac{\lambda_\Phi}{4}\left(\Phi^\dagger\Phi - \frac{v_\Phi^2}{2}\right)^2 - \lambda_{H\Phi}\left(H^\dagger H - \frac{v_H^2}{2}\right)\left(\Phi^\dagger\Phi - \frac{v_\Phi^2}{2}\right),$$

$X_\mu \equiv V_\mu$ here

$$\Phi(x) = (v_\phi + \phi(x))/\sqrt{2}$$

- There appear a new singlet scalar (**dark Higgs**) $\phi(x)$ from $\Phi(x)$, which mixes with the SM Higgs boson through Higgs portal interaction ($\lambda_{H\Phi}$ term)
- The effects must be similar to the singlet scalar in the fermion CDM model, and generically true in the DM with dark gauge symmetry
- Can accommodate GeV scale gamma ray excess from GC with $VV \rightarrow \phi\phi$
- **Can modify the Higgs inflation : No tight correlation with top mass**

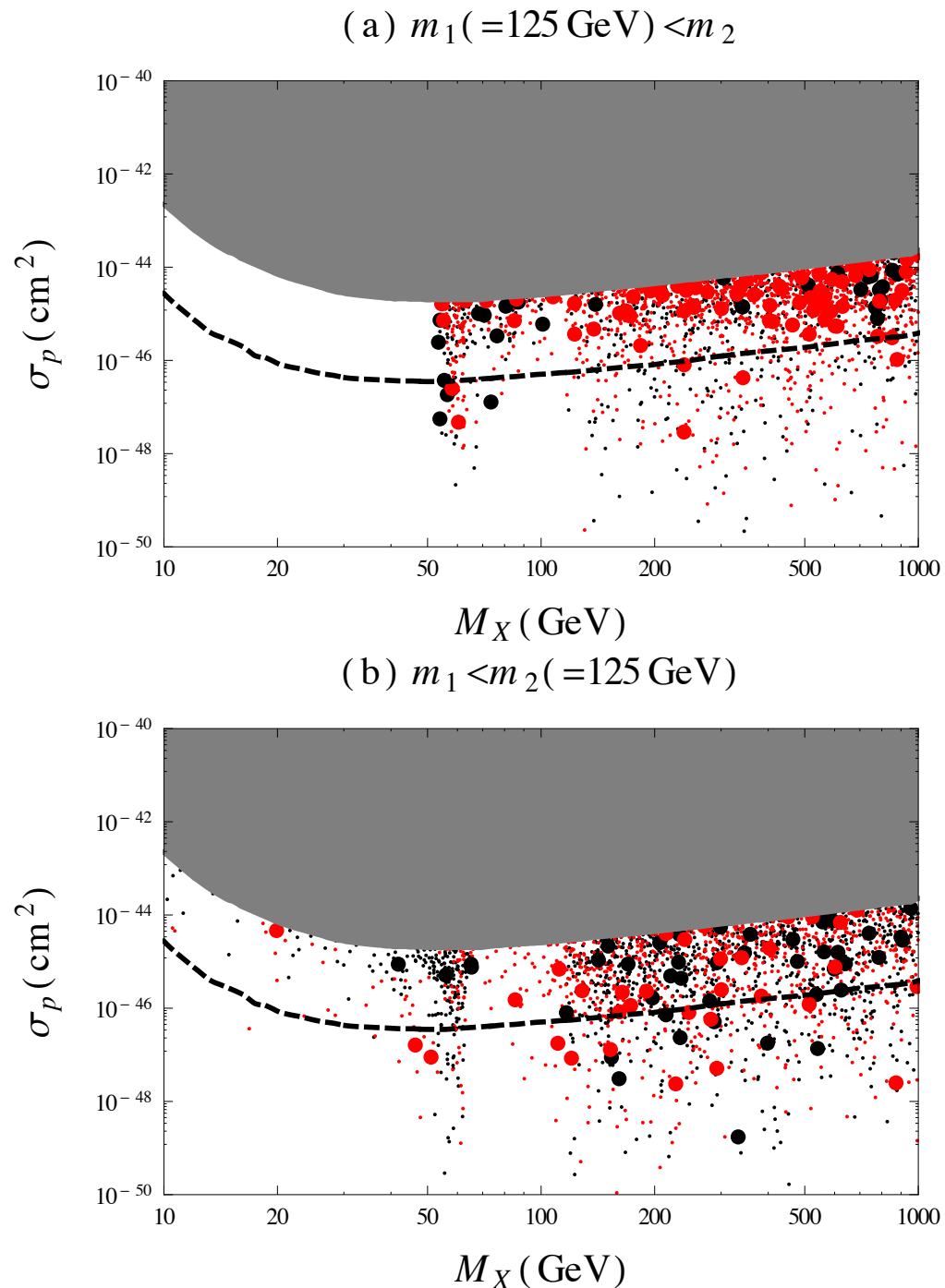


Figure 6. The scattered plot of σ_p as a function of M_X . The big (small) points (do not) satisfy the WMAP relic density constraint within 3σ , while the red-(black-)colored points gives $r_1 > 0.7$ ($r_1 < 0.7$). The grey region is excluded by the XENON100 experiment. The dashed line denotes the sensitivity of the next XENON experiment, XENON1T.

New scalar (Dark Higgs)
improves EW vacuum stability

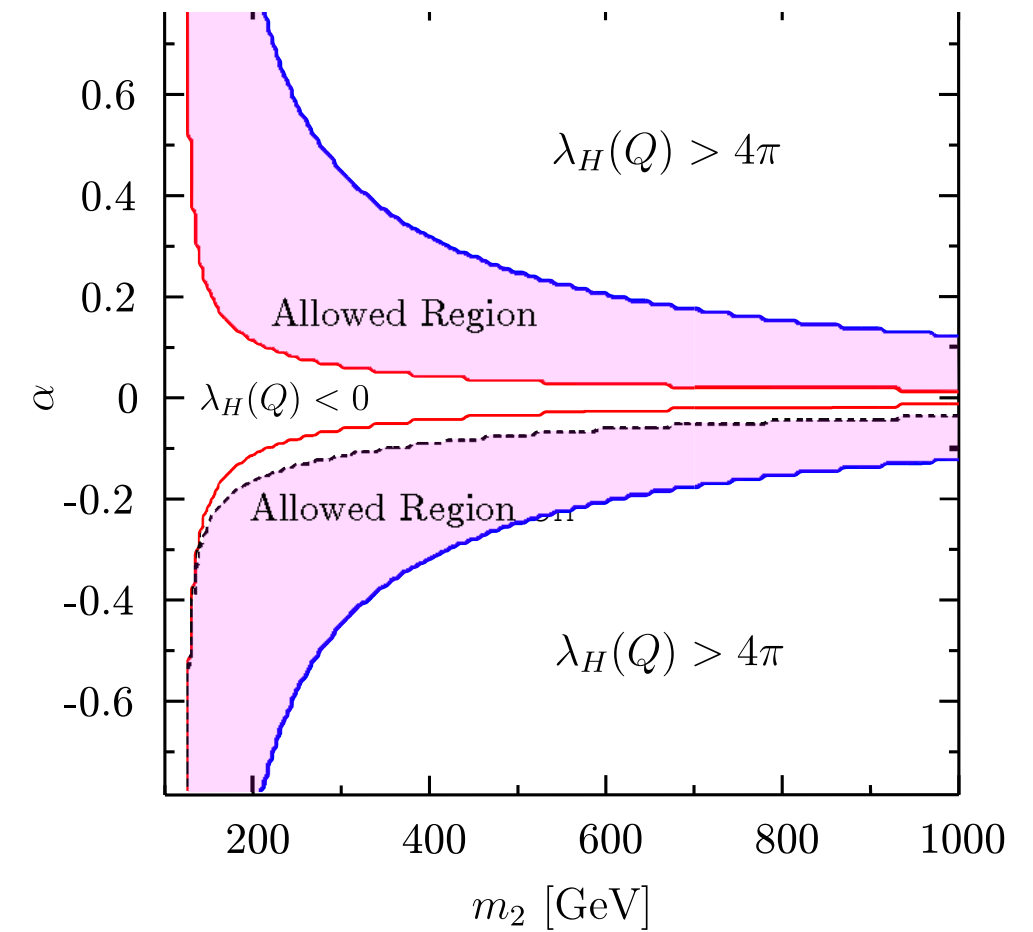


Figure 8. The vacuum stability and perturbativity constraints in the α - m_2 plane. We take $m_1 = 125 \text{ GeV}$, $g_X = 0.05$, $M_X = m_2/2$ and $v_\Phi = M_X/(g_X Q_\Phi)$.

Interaction Lagrangians

Scalar DM

$$\mathcal{L}_{\text{SDM}}^{\text{int}} = -h \left(\frac{2m_W^2}{v_h} W_\mu^+ W^{-\mu} + \frac{m_Z^2}{v_h} Z_\mu Z^\mu \right) - \lambda_{HS} v_h h S^2.$$

Singlet FDM

$$\begin{aligned} \mathcal{L}_{\text{FDM}}^{\text{int}} = & - (H_1 \cos \alpha + H_2 \sin \alpha) \left(\sum_f \frac{m_f}{v_h} \bar{f} f - \frac{2m_W^2}{v_h} W_\mu^+ W^{-\mu} - \frac{m_Z^2}{v_h} Z_\mu Z^\mu \right) \\ & + g_\chi (H_1 \sin \alpha - H_2 \cos \alpha) \bar{\chi} \chi . \end{aligned}$$

Vector DM

$$\begin{aligned} \mathcal{L}_{\text{VDM}}^{\text{int}} = & - (H_1 \cos \alpha + H_2 \sin \alpha) \left(\sum_f \frac{m_f}{v_h} \bar{f} f - \frac{2m_W^2}{v_h} W_\mu^+ W^{-\mu} - \frac{m_Z^2}{v_h} Z_\mu Z^\mu \right) \\ & - \frac{1}{2} g_V m_V (H_1 \sin \alpha - H_2 \cos \alpha) V_\mu V^\mu . \end{aligned}$$

NB: One can not simply ignore 125 GeV Higgs Boson or singlet scalar by hand, since it would violate gauge invariance and unitarity !

- EFT : Effective operator $\mathcal{L}_{int} = \frac{m_q}{\Lambda_{dd}^3} \bar{q}q\bar{\chi}\chi$
- S.M.: Simple scalar mediator S of

$$\mathcal{L}_{int} = \left(\frac{m_q}{v_H} \sin \alpha \right) S \bar{q}q - \lambda_s \cos \alpha S \bar{\chi}\chi$$
- H.M.: A case where a Higgs is a mediator

$$\mathcal{L}_{int} = - \left(\frac{m_q}{v_H} \cos \alpha \right) H \bar{q}q - \lambda_s \sin \alpha H \bar{\chi}\chi$$
- H.P.: Higgs portal model as in eq. (2).

$$\frac{d\sigma_i}{dm_{\chi\chi}} \propto \left| \frac{\sin 2\alpha g_\chi}{m_{\chi\chi}^2 - m_{H_1}^2 + im_{H_1}\Gamma_{H_1}} - \frac{\sin 2\alpha g_\chi}{m_{\chi\chi}^2 - m_{H_2}^2 + im_{H_2}\Gamma_{H_2}} \right|^2$$

H.P. $\xrightarrow[m_{H_2}^2 \gg \hat{s}]{} \text{H.M.},$

S.M. $\xrightarrow[m_S^2 \gg \hat{s}]{} \text{EFT},$

H.M. $\neq \text{EFT}.$

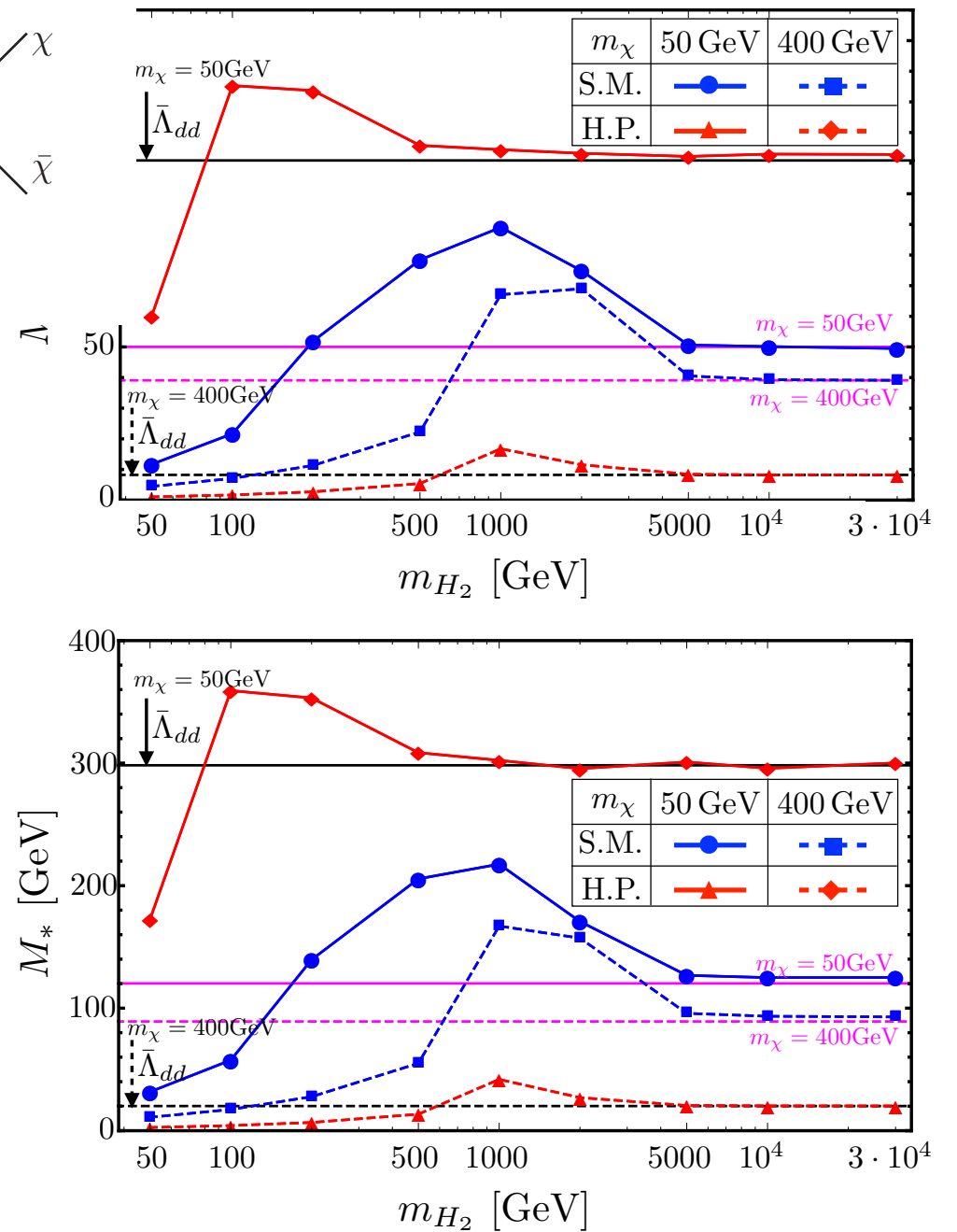
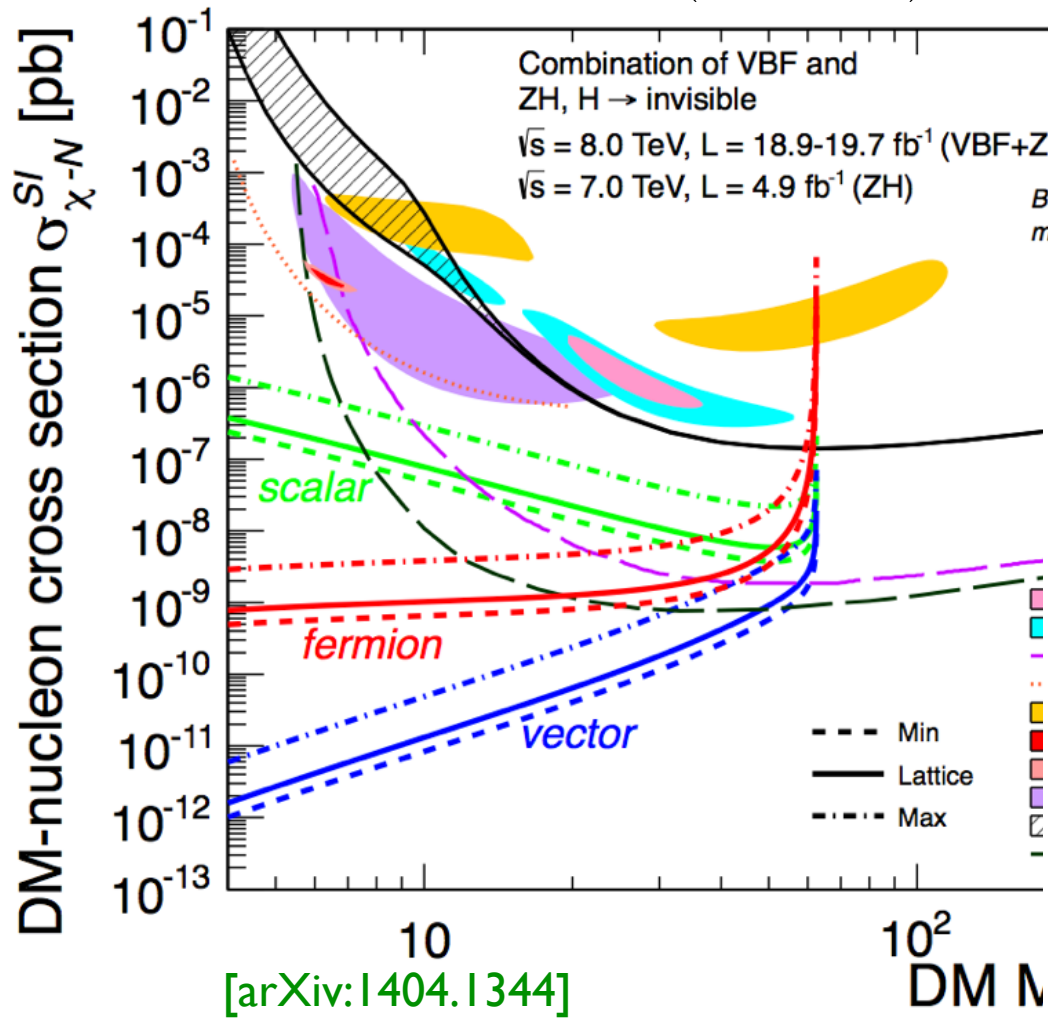


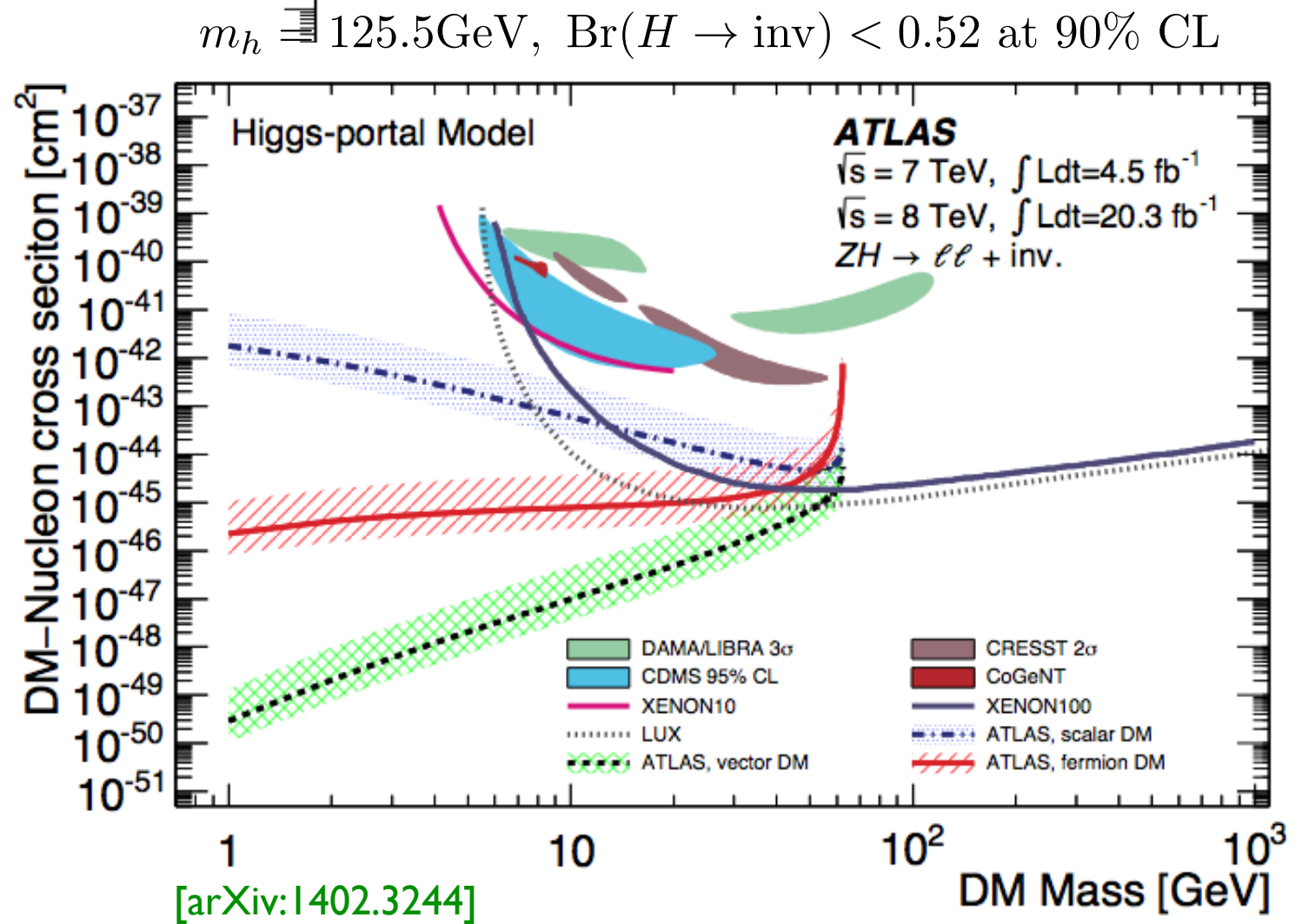
FIG. 3: The experimental bounds on M_* at 90% C.L. as a function of m_{H_2} (m_S in S.M. case) in the monojet+ \cancel{E}_T search (upper) and $t\bar{t} + \cancel{E}_T$ search (lower). Each line corresponds to the EFT approach (magenta), S.M. (blue), H.M. (black), and H.P. (red), respectively. The bound of S.M., H.M., and H.P., are expressed in terms of the effective mass M_* through the Eq.(16)-(20). The solid and dashed lines correspond to $m_\chi = 50$ GeV and 400 GeV in each model, respectively.

Collider Implications

$m_h = 125\text{GeV}$, $\text{Br}(H \rightarrow \text{inv}) < 0.51$ at 90% CL



Based on EFTs



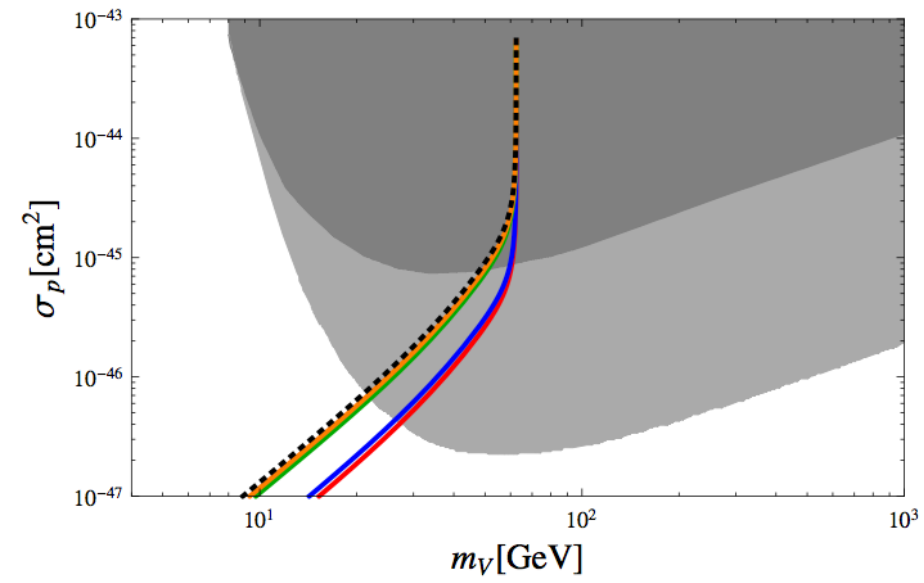
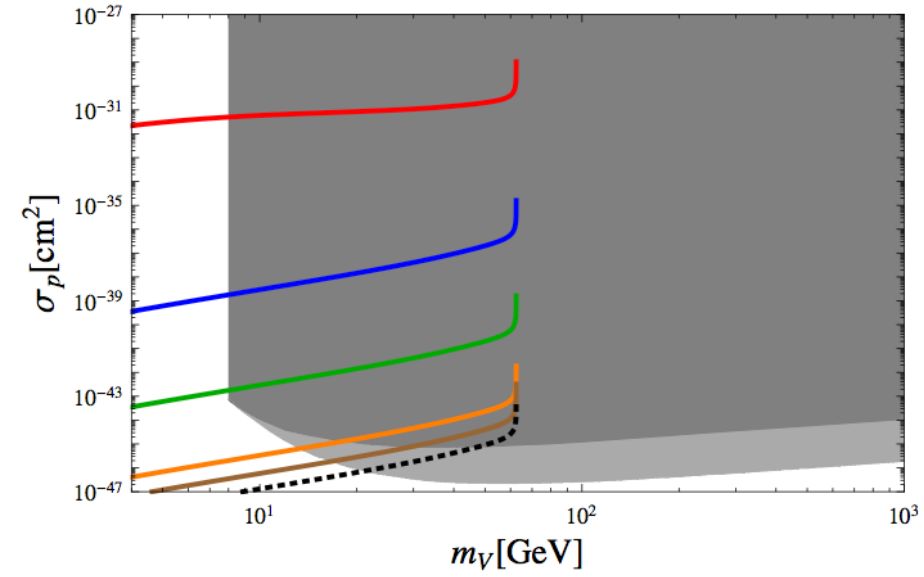
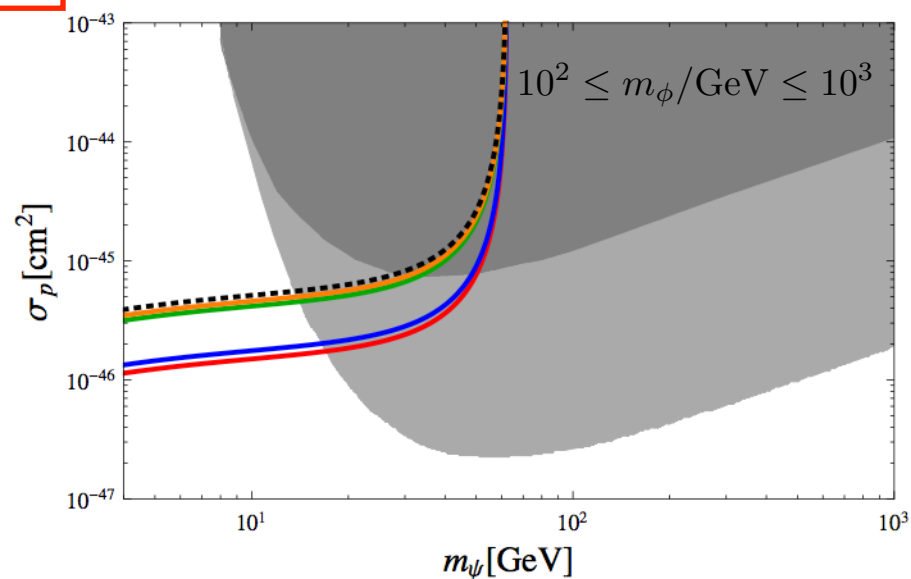
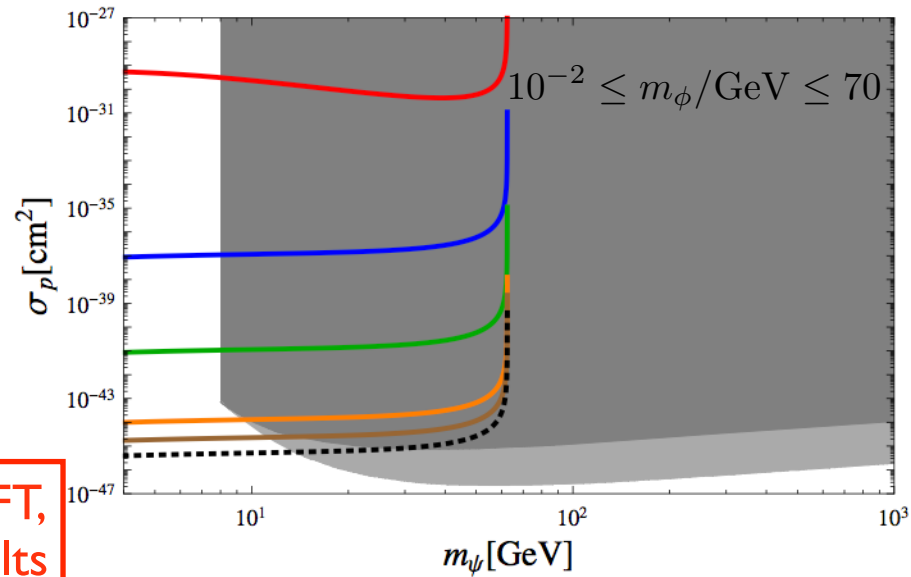
- However, in renormalizable unitary models of Higgs portals, **2 more relevant parameters !**

$$\begin{aligned}\mathcal{L}_{\text{SFDM}} = & \bar{\psi} (i\partial - m_\psi - \lambda_\psi S) - \mu_{HS} S H^\dagger H - \frac{\lambda_{HS}}{2} S^2 H^\dagger H \\ & + \frac{1}{2} \partial_\mu S \partial^\mu S - \frac{1}{2} m_S^2 S^2 - \mu'_S S - \frac{\mu'_S}{3} S^3 - \frac{\lambda_S}{4} S^4.\end{aligned}$$

[arXiv: 1405.3530, S. Baek, P. Ko & WIPark, PRD]

$$\begin{aligned}\sigma_p^{\text{SI}} = & (\sigma_p^{\text{SI}})_{\text{EFT}} c_\alpha^4 m_h^4 \mathcal{F}(m_{\text{DM}}, \{m_i\}, v) \\ \simeq & (\sigma_p^{\text{SI}})_{\text{EFT}} c_\alpha^4 \left(1 - \frac{m_h^2}{m_2^2}\right)^2\end{aligned}$$

$$\mathcal{L}_{\text{VDM}} = -\frac{1}{4} V_{\mu\nu} V^{\mu\nu} + D_\mu \Phi^\dagger D^\mu \Phi - \lambda_\Phi \left(\Phi^\dagger \Phi - \frac{v_\Phi^2}{2}\right)^2 - \lambda_{\Phi H} \left(\Phi^\dagger \Phi - \frac{v_\Phi^2}{2}\right) \left(H^\dagger H - \frac{v_H^2}{2}\right)$$



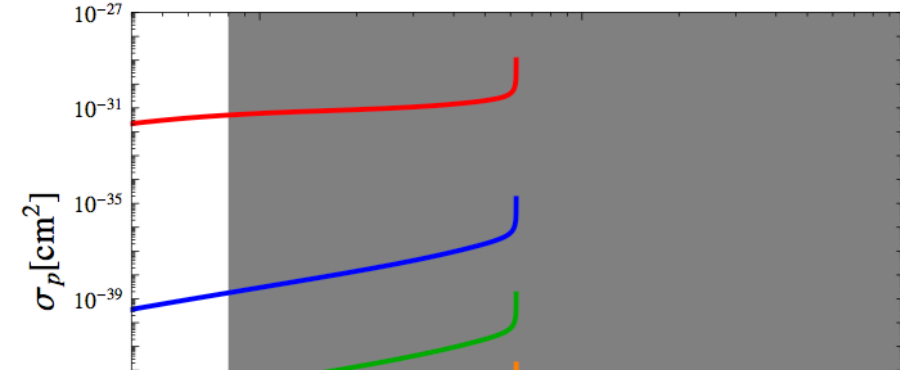
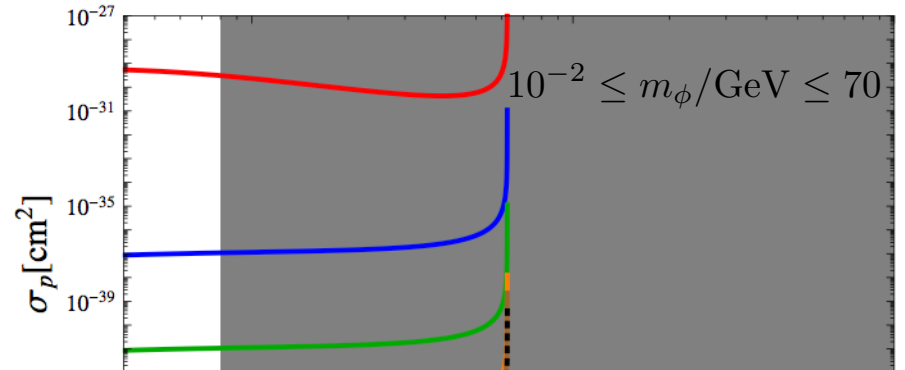
- However, in renormalizable unitary models of Higgs portals, **2 more relevant parameters !**

$$\begin{aligned}\mathcal{L}_{\text{SFDM}} = & \bar{\psi} (i\partial - m_\psi - \lambda_\psi S) - \mu_{HS} S H^\dagger H - \frac{\lambda_{HS}}{2} S^2 H^\dagger H \\ & + \frac{1}{2} \partial_\mu S \partial^\mu S - \frac{1}{2} m_S^2 S^2 - \mu'_S S - \frac{\mu'_S}{3} S^3 - \frac{\lambda_S}{4} S^4.\end{aligned}$$

[arXiv: 1405.3530, S. Baek, P. Ko & WIPark, PRD]

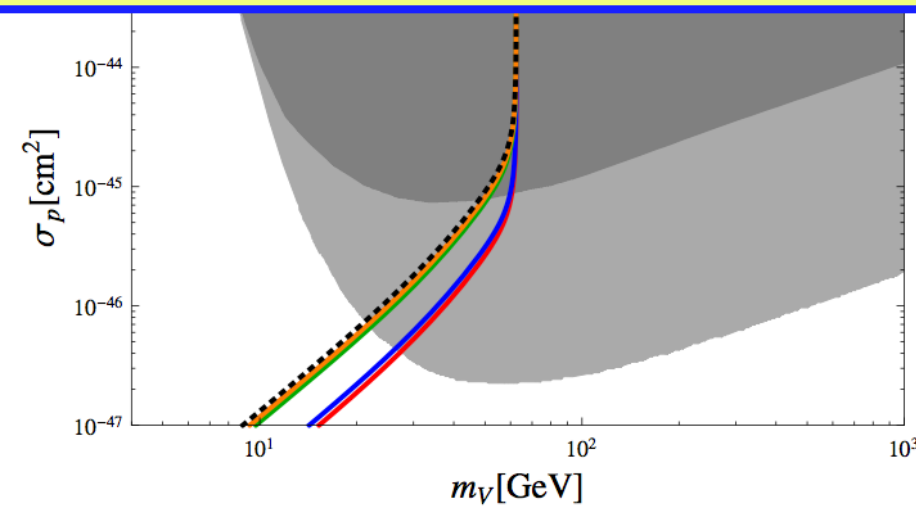
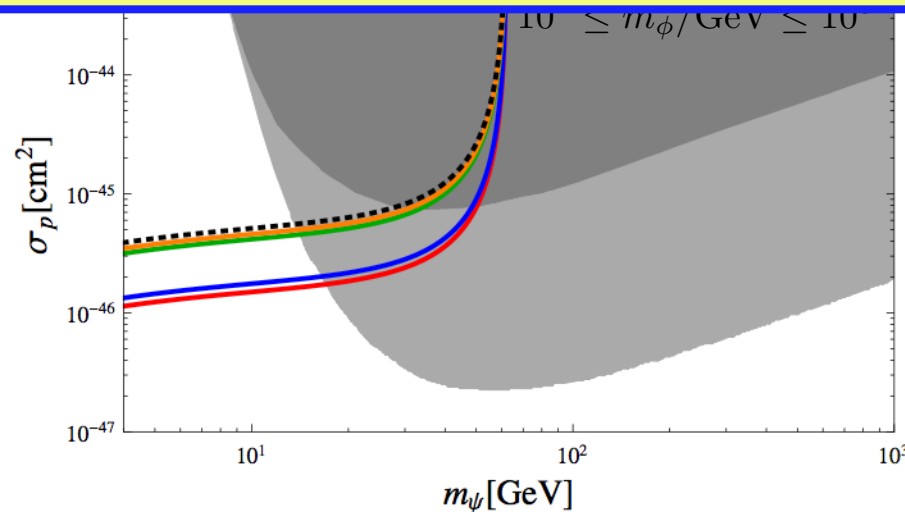
$$\begin{aligned}\sigma_p^{\text{SI}} = & (\sigma_p^{\text{SI}})_{\text{EFT}} c_\alpha^4 m_h^4 \mathcal{F}(m_{\text{DM}}, \{m_i\}, v) \\ \simeq & (\sigma_p^{\text{SI}})_{\text{EFT}} c_\alpha^4 \left(1 - \frac{m_h^2}{m_2^2}\right)^2\end{aligned}$$

$$\mathcal{L}_{\text{VDM}} = -\frac{1}{4} V_{\mu\nu} V^{\mu\nu} + D_\mu \Phi^\dagger D^\mu \Phi - \lambda_\Phi \left(\Phi^\dagger \Phi - \frac{v_\Phi^2}{2}\right)^2 - \lambda_{\Phi H} \left(\Phi^\dagger \Phi - \frac{v_\Phi^2}{2}\right) \left(H^\dagger H - \frac{v_H^2}{2}\right)$$



Dashed curve
ATLAS,CMS

Interpretation of collider data is quite model-dependent in Higgs portal DMs and in general



Invisible H decay into a pair of VDM

[arXiv: 1405.3530, S. Baek, P. Ko & WIPark, PRD]

$$(\Gamma_h^{\text{inv}})_{\text{EFT}} = \frac{\lambda_{VH}^2}{128\pi} \frac{v_H^2 m_h^3}{m_V^4} \times \left(1 - \frac{4m_V^2}{m_h^2} + 12 \frac{m_V^4}{m_h^4}\right) \left(1 - \frac{4m_V^2}{m_h^2}\right)^{1/2} \quad (23)$$

Diverge when
 $m_V \rightarrow 0 !!$

$$m_V \propto g_x Q_\Phi v_\Phi$$

$$\frac{g_X^2}{m_V^2} = \frac{g_X^2}{g_X^2 Q_\Phi^2 v_\Phi^2} \rightarrow \frac{1}{v_\Phi^2} = \text{finite}$$

VS.

$$\Gamma_i^{\text{inv}} = \frac{g_X^2}{32\pi} \frac{m_i^3}{m_V^2} \left(1 - \frac{4m_V^2}{m_i^2} + 12 \frac{m_V^4}{m_i^4}\right) \left(1 - \frac{4m_V^2}{m_i^2}\right)^{1/2} \sin^2 \alpha \quad (22)$$

Invisible H decay width : finite for small mV
 in unitary/renormalizable model

Two Limits for $m_V \rightarrow 0$

**Also see the addendum:
by S Baek, P Ko, WI Park**

- $m_V = g_X Q_\Phi v_\Phi$ in the UV completion with dark Higgs boson
- Case I : $g_X \rightarrow 0$ with finite $v_\Phi \neq 0$

$$\frac{g_X^2 Q_\Phi^2}{m_V^2} = \frac{g_X^2 Q_\Phi^2}{g_X^2 Q_\Phi^2 v_\Phi^2} = \frac{1}{v_\Phi^2} = \text{finite.}$$

$$(\Gamma_h^{\text{inv}})_{\text{UV}} = \frac{1}{32\pi} \frac{m_h^3}{v_\Phi^2} \sin^2 \alpha = \Gamma(h \rightarrow a_\Phi a_\Phi)$$

with a_Φ being the NG boson for spontaneously broken global $U(1)_X$

- Case II : $v_\Phi \rightarrow 0$ with finite $g_X \neq 0$

$$\alpha \xrightarrow{v_\Phi \rightarrow 0^+} \frac{2\lambda_{H\Phi} v_\Phi}{\lambda_H v_H}$$

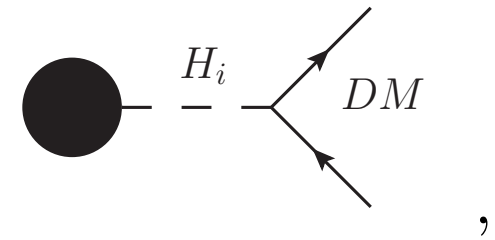
$$\frac{g_X^2 Q_\Phi^2}{m_V^2} \sin^2 \alpha \xrightarrow{v_\Phi \rightarrow 0^+} \frac{4\lambda_{H\Phi}^2}{\lambda_H^2 v_H^2} = \frac{2\lambda_{H\Phi}^2}{\lambda_H m_h^2} = \text{finite,}$$

$$(\Gamma_h^{\text{inv}})_{\text{UV}} \xrightarrow{v_\Phi \rightarrow 0^+} \frac{1}{16\pi} \frac{\lambda_{H\Phi}^2 m_h}{\lambda_H}$$

Therefore $\Gamma(h \rightarrow VV)$ is finite when $m_V \rightarrow 0$ in the UV completions

DM Production @ ILC

P Ko, H Yokoya, arXiv:1603.08802, JHEP



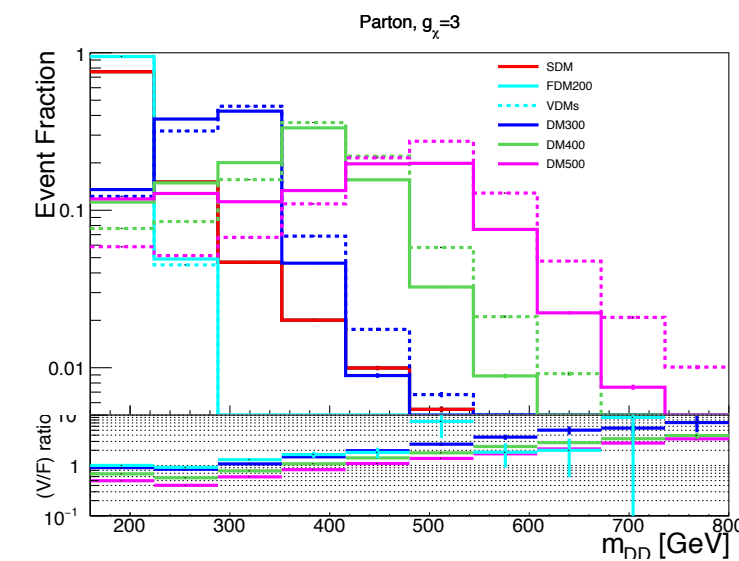
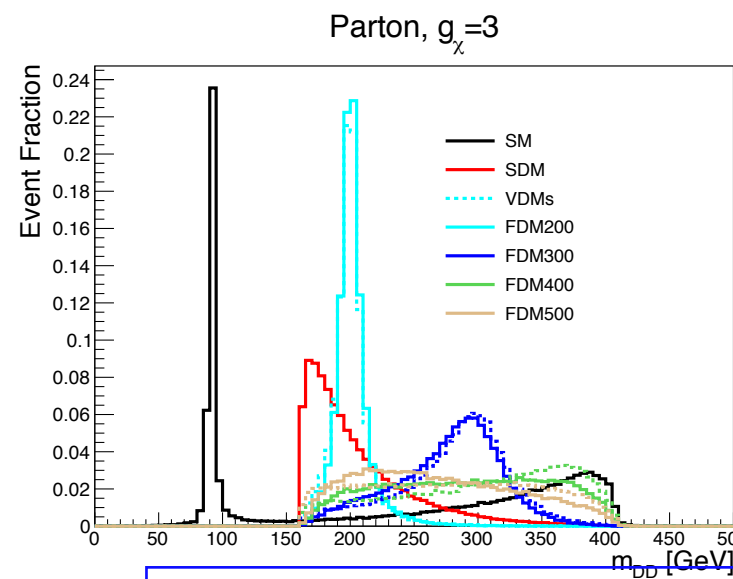
$$t \equiv m_{DD}^2$$

We consider $e^+e^- \rightarrow Z^* \rightarrow ZH_{i=1,2}$
followed by $H_i \rightarrow \bar{\chi}\chi$

$$\frac{d\sigma_{\text{SDM}}}{dt} \propto \sigma_{\text{SDM}}^{h^*} \times \left| \frac{1}{t - m_h^2 + im_h\Gamma_h} \right|^2,$$

$$\frac{d\sigma_{\text{FDM}}}{dt} \propto \sigma_{\text{FDM}}^{h^*} \times \left| \frac{1}{t - m_{H_1}^2 + im_{H_1}\Gamma_{H_1}} - \frac{1}{t - m_{H_2}^2 + im_{H_2}\Gamma_{H_2}} \right|^2 \cdot (2t - 8m_\chi^2),$$

$$\frac{d\sigma_{\text{VDM}}}{dt} \propto \sigma_{\text{VDM}}^{h^*} \times \left| \frac{1}{t - m_{H_1}^2 + im_{H_1}\Gamma_{H_1}} - \frac{1}{t - m_{H_2}^2 + im_{H_2}\Gamma_{H_2}} \right|^2 \cdot \left(2 + \frac{(t - 2m_D^2)^2}{4m_V^4} \right).$$



Fix DM mass = 80 GeV, $\sin(\alpha) = 0.3$,
and vary H2 mass (200,300,400,500) GeV

Asymptotic behavior in the full theory ($t \equiv m_{\chi\chi}^2$)

ScalarDM : $G(t) \sim \frac{1}{(t - m_H^2)^2 + m_H^2 \Gamma_H^2}$ (5.7)

SFDM : $G(t) \sim \left| \frac{1}{t - m_1^2 + im_1\Gamma_1} - \frac{1}{t - m_2^2 + im_2\Gamma_2} \right|^2 (t - 4m_\chi^2)$ (5.8)

$$\rightarrow |\frac{1}{t^2}|^2 \times t \sim \frac{1}{t^3} \text{ (as } t \rightarrow \infty)$$
 (5.9)

VDM : $G(t) \sim \left| \frac{1}{t - m_1^2 + im_1\Gamma_1} - \frac{1}{t - m_2^2 + im_2\Gamma_2} \right|^2 \left[2 + \frac{(t - 2m_V^2)^2}{4m_V^4} \right]$ (5.10)

$$\rightarrow |\frac{1}{t^2}|^2 \times t^2 \sim \frac{1}{t^2} \text{ (as } t \rightarrow \infty)$$
 (5.11)

Asymptotic behavior w/o the 2nd Higgs (EFT)

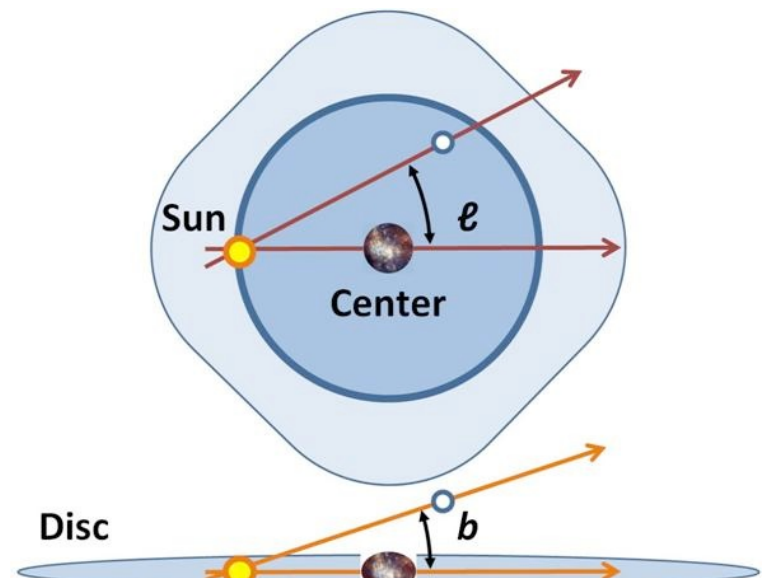
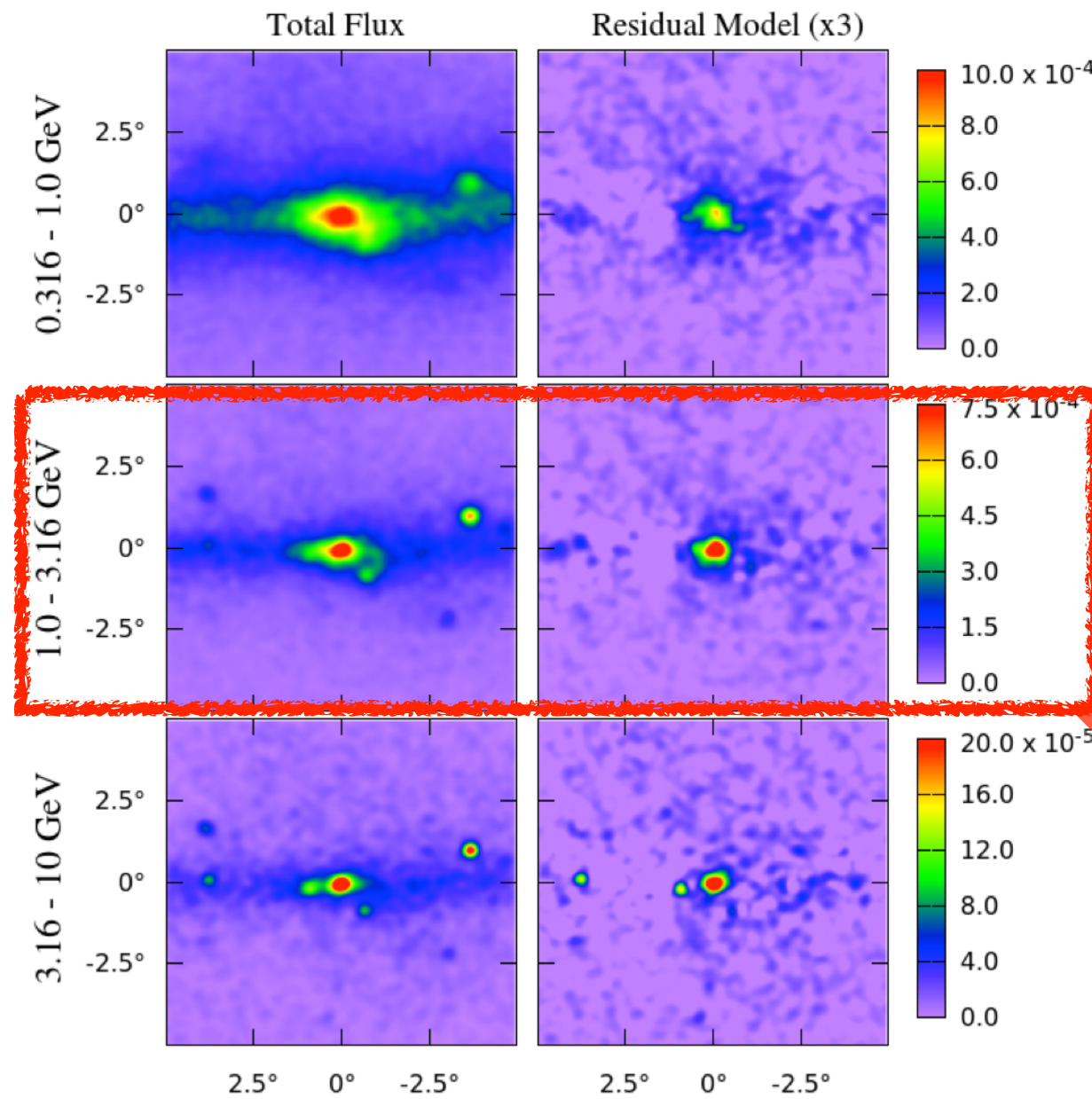
SFDM : $G(t) \sim \frac{1}{(t - m_H^2)^2 + m_H^2 \Gamma_H^2} (t - 4m_\chi^2)$
 $\rightarrow \frac{1}{t}$ (as $t \rightarrow \infty$)

Unitarity is violated in EFT!

VDM : $G(t) \sim \frac{1}{(t - m_H^2)^2 + m_H^2 \Gamma_H^2} \left[2 + \frac{(t - 2m_V^2)^2}{4m_V^4} \right]$
 $\rightarrow \text{constant (as } t \rightarrow \infty)$

Fermi-LAT GC γ -ray

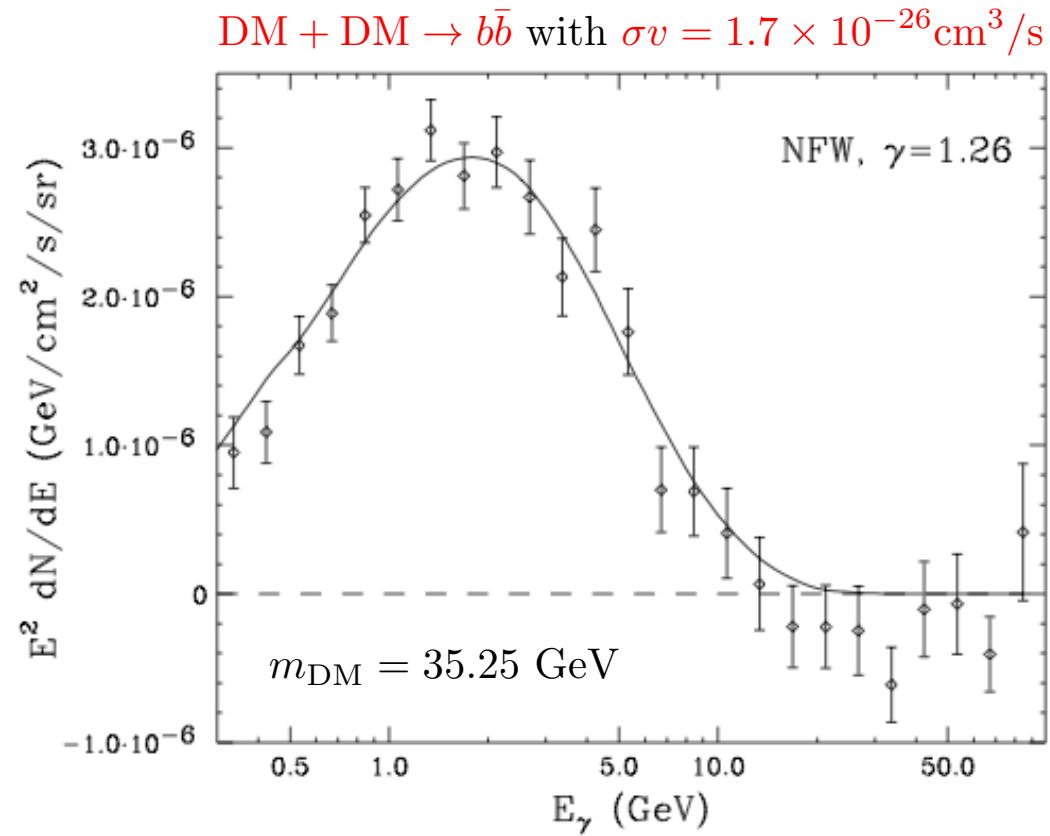
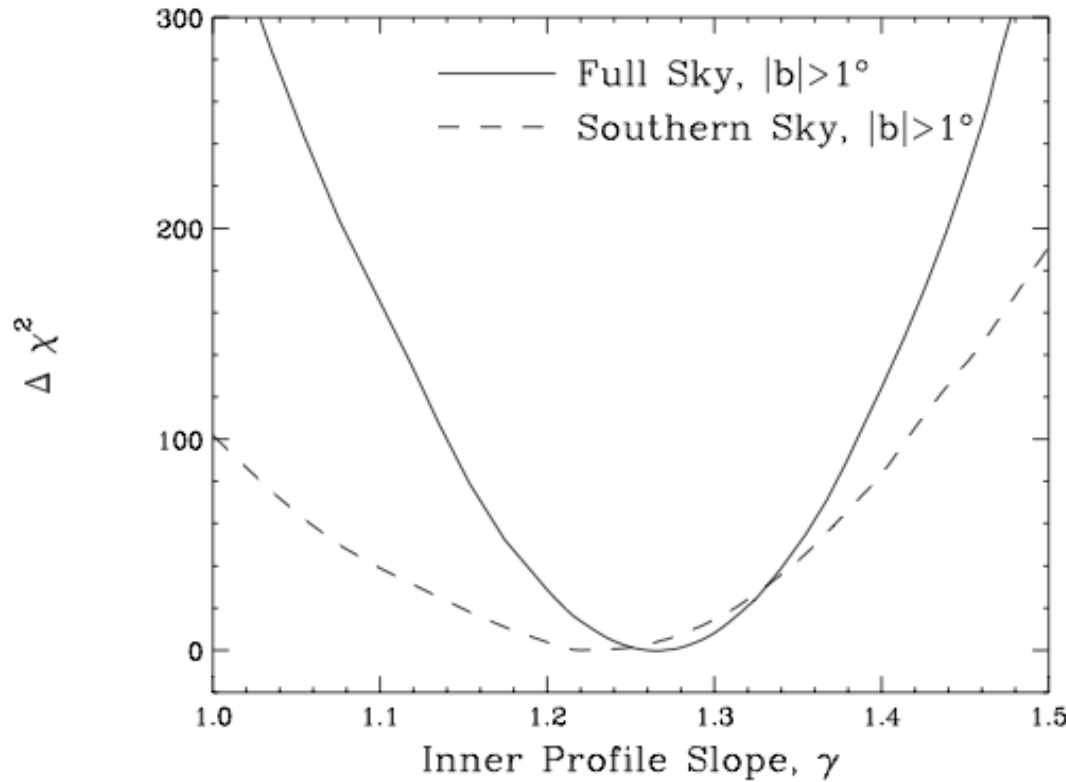
see arXiv:1612.05687 for a recent overview by
C.Karwin, S. Murgia, T.Tait, T.A.Porter,P.Tanedo



GC : $b \sim l \lesssim 0.1^\circ$

extended
GeV scale excess!

● A DM interpretation



* See “I402.6703, T. Daylan et.al.” for other possible channels

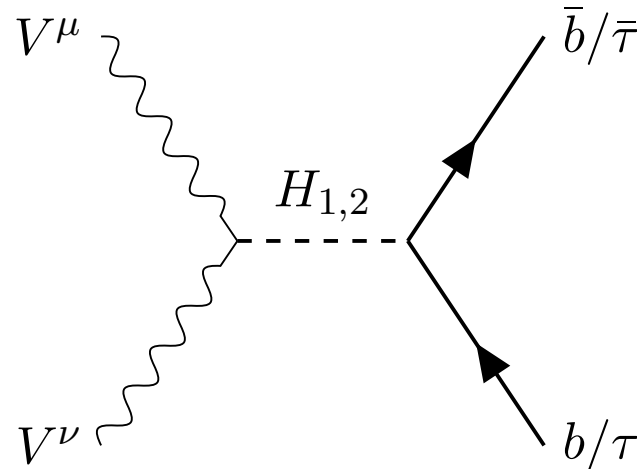
● Millisecond Pulsars (astrophysical alternative)

- It may or may not be the main source, depending on
 - luminosity func.
 - bulge population
 - distribution of bulge population

* See “I404.2318, Q. Yuan & B. Zhang” and “I407.5625, I. Cholis, D. Hooper & T. Linden”

GC gamma ray in HP VDM

P.Ko,WI Park,Y.Tang. arXiv:1404.5257, JCAP



H2 : 125 GeV Higgs
H1 : absent in EFT

Figure 2. Dominant s channel $b + \bar{b}$ (and $\tau + \bar{\tau}$) production

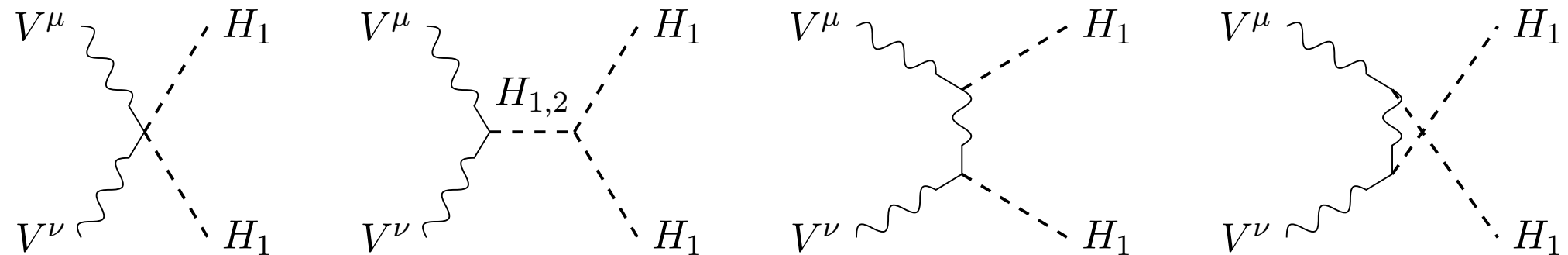


Figure 3. Dominant s/t -channel production of H_1 s that decay dominantly to $b + \bar{b}$

Importance of HP VDM with Dark Higgs Boson

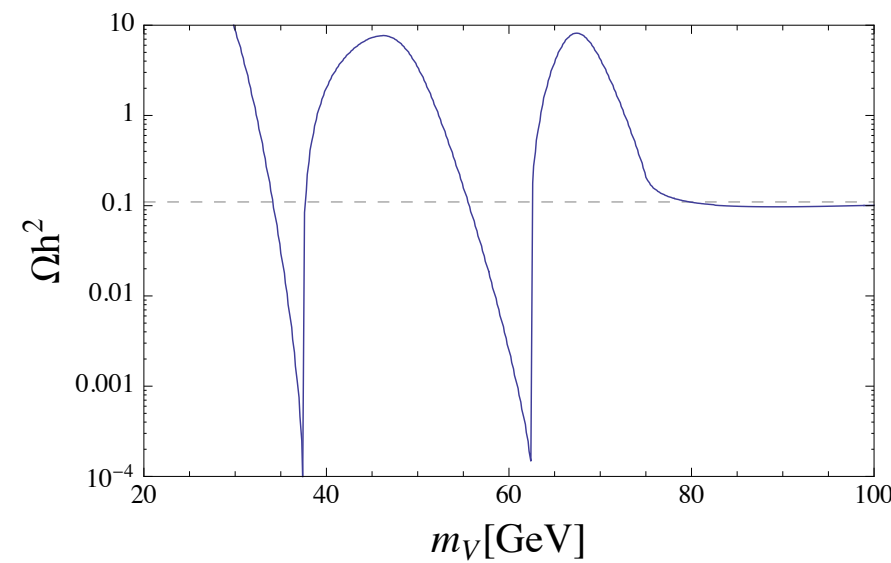


Figure 4. Relic density of dark matter as function of m_ψ for $m_h = 125$, $m_\phi = 75$ GeV, $g_X = 0.2$, and $\alpha = 0.1$.

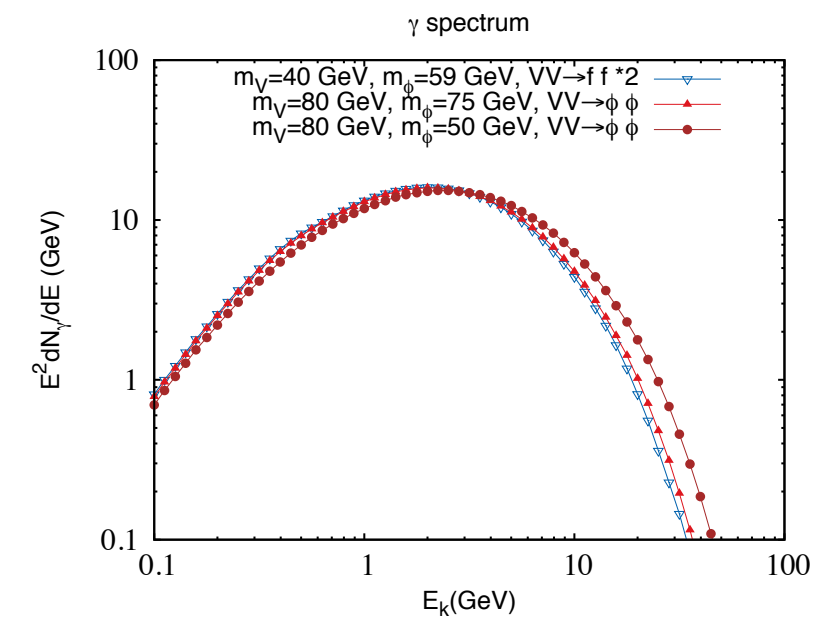


Figure 5. Illustration of γ spectra from different channels. The first two cases give almost the same spectra while in the third case γ is boosted so the spectrum is shifted to higher energy.

This mass range of VDM would have been
impossible in the VDM model (EFT)

And No 2nd neutral scalar (Dark Higgs) in EFT

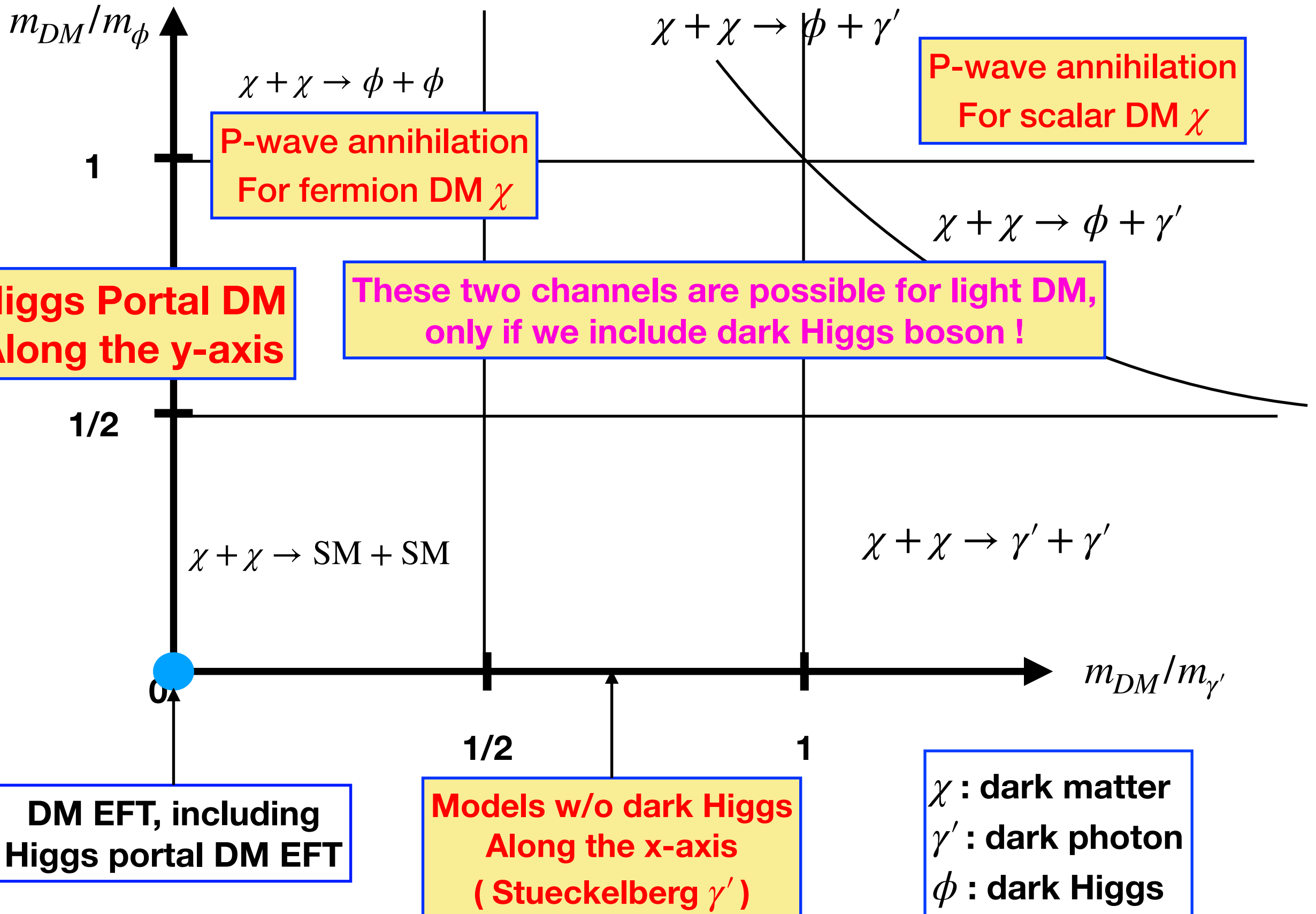
Summary

- Phenomenology of HP VDM and Singlet FDM presented within EFT vs. UV completed models
- EFT approach has a number of drawbacks : non-renormalizable, unitarity violation at high energy colliders, and it applies only if $m_{DM}, m_{SM} \ll m_\phi$ [But we don't know mass scales of dark particles !]
- In particular, one has $\Gamma_{\text{EFT}}(H_{125} \rightarrow VV) \rightarrow \infty$, as $m_V \rightarrow 0$, whereas it is finite in UV completed models [Importance of gauge invariance, unitarity and renormalizability]
- The dark Higgs ϕ can play crucial roles in interpreting the DM signatures at colliders, explaining the GC γ -ray excess ($VV \rightarrow \phi\phi$), improving vacuum stability up to Planck scale, modifying the Higgs inflation [ϕ should be actively searched for !]

Uncovered Topics

- Dark Higgs contribution to the DM bound state (PK, T. Matsui, Yi-Lei Tang, (2019)) [Talk by Kalliopi Petraki]
- Dark Higgs effects on Higgs inflation (J.Kim,PK. W.Park (2014), Khan, J.Kim, PK(2023)): $R(\xi_H H^\dagger H + \xi_\phi \phi^\dagger \phi)$
- SIDM (DM-DM interactions): light mediators (either ϕ or Z').....
- DM-DR interaction: H_0 & σ_8 puzzles (PK,Yong Tang, (2016) 2 papers,+Nagata(2027))
- In short, dark Higgs can play crucial roles in both (astro)particle physics and cosmology

Dark sector parameter space for a fixed m_{DM}



$U(1)_{L_\mu - L_\tau}$ -charged DM

: Z' only vs. $Z' + \phi$

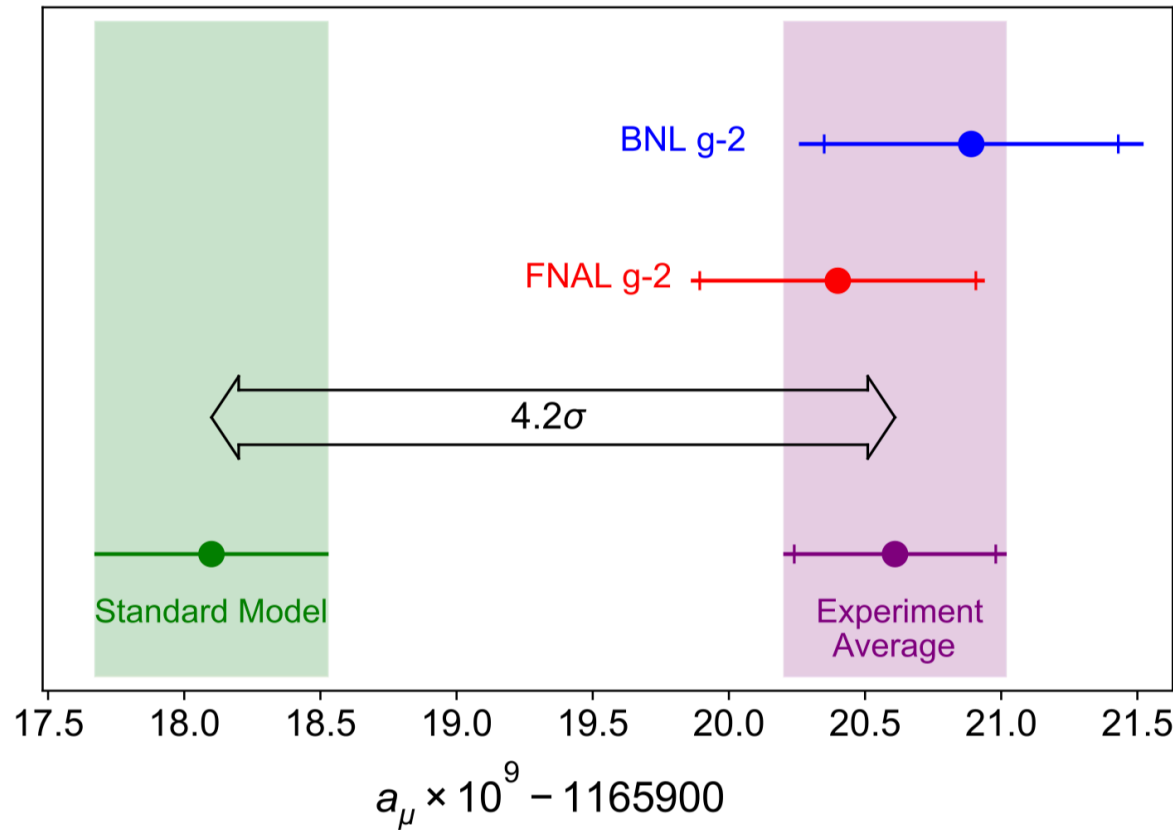
cf: Let me call Z' , $U(1)_{L_\mu - L_\tau}$ gauge boson,
“dark photon”, since it couples to DM

SM+ $U(1)_{L_\mu-L_\tau}$ gauge sym

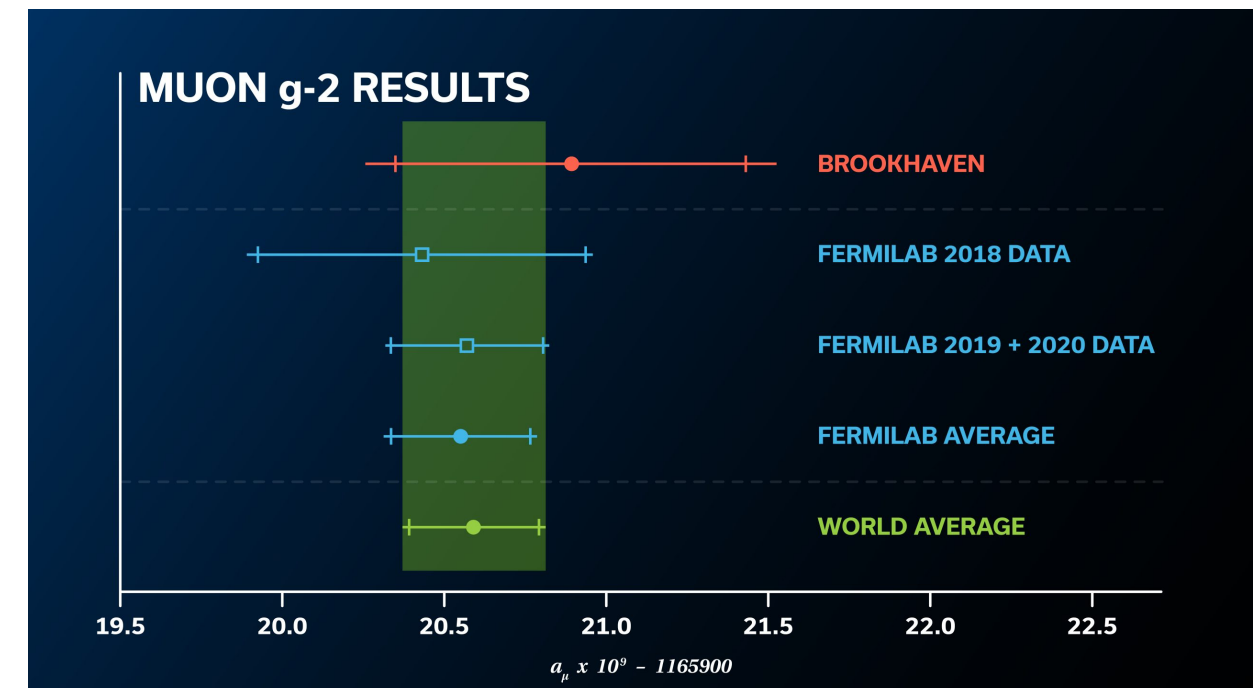
- He, Josh, Lew, Volkas, PRD 43, 22; PRD 44, 2118 (1991)
- One of the anomaly free gauge groups without extension of fermion contents
- The simplest anomaly free $U(1)$ extensions that couple to the SM fermions directly
- Can affect the muon g-2, PAMELA e^+ excess, **(and B anomalies with extra fermions : Not covered in this talk)**

Muon g-2

Talk by Dominik Stoeckinger



The Muon g-2 Collaboration, 2104.03281



Announcement on Aug 10, 2023

Excellent example for graduate students

- Relativistic E&M (spinning particle in EM fields)
- Special relativity (time dilation)
- (V-A) structure of charged weak interaction

Muon (g-2) in $U(1)_{\mu-\tau}$ Model

Baek, Deshpande, He, Ko : hep-ph/0104141
 Baek, Ko : arXiv:0811.1646 [hep-ph]

$$\begin{aligned} L_L^e &: (1, 2, -1)(0) & e_R &: (1, 1, -2)(0) \\ L_L^\mu &: (1, 2, -1)(2a) & \mu_R &: (1, 1, -2)(2a) \\ L_L^\tau &: (1, 2, -1)(-2a) & \mu_R &: (1, 1, -2)(-2a). \end{aligned}$$

$$\Delta a_\mu = \frac{\alpha'}{2\pi} \int_0^1 dx \frac{2m_\mu^2 x^2 (1-x)}{x^2 m_\mu^2 + (1-x) M_{Z'}^2} \approx \frac{\alpha'}{2\pi} \frac{2m_\mu^2}{3M_{Z'}^2}$$

$$Z' \rightarrow \mu^+ \mu^-, \tau^+ \tau^-, \nu_\alpha \bar{\nu}_\alpha \text{ (with } \alpha = \mu \text{ or } \tau), \psi_D \bar{\psi}_D$$

$$\Gamma(Z' \rightarrow \mu^+ \mu^-) = \Gamma(Z' \rightarrow \tau^+ \tau^-) = 2\Gamma(Z' \rightarrow \nu_\mu \bar{\nu}_\mu) = 2\Gamma(Z' \rightarrow \nu_\tau \bar{\nu}_\tau) = \Gamma(Z' \rightarrow \psi_D \bar{\psi}_D)$$

if $M_{Z'} \gg m_\mu, m_\tau, M_{\text{DM}}$. The total decay rate of Z' is approximately given by

$$\Gamma_{\text{tot}}(Z') = \frac{\alpha'}{3} M_{Z'} \times 4(3) \approx \frac{4(\text{or } 3)}{3} \text{ GeV} \left(\frac{\alpha'}{10^{-2}} \right) \left(\frac{M_{Z'}}{100 \text{ GeV}} \right)$$

$$\begin{aligned} q\bar{q} \text{ (or } e^+ e^-) &\rightarrow \gamma^*, Z^* \rightarrow \mu^+ \mu^- Z', \tau^+ \tau^- Z' \\ &\rightarrow Z^* \rightarrow \nu_\mu \bar{\nu}_\mu Z', \nu_\tau \bar{\nu}_\tau Z' \end{aligned}$$

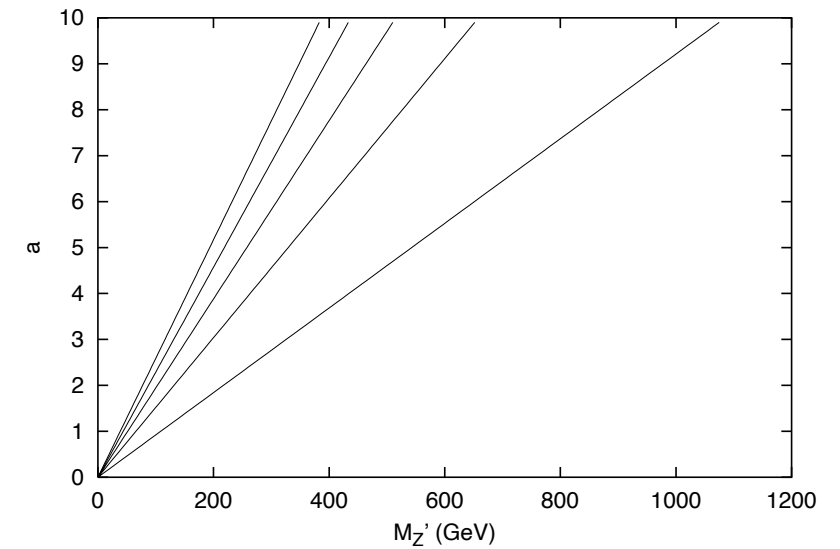
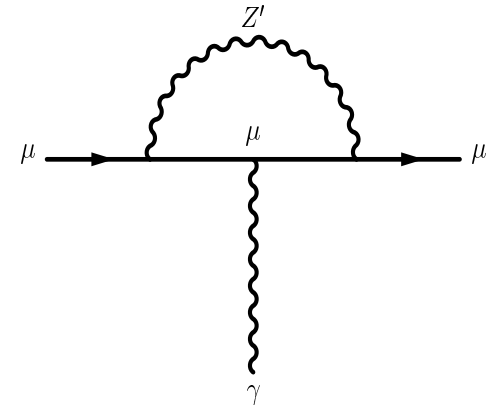
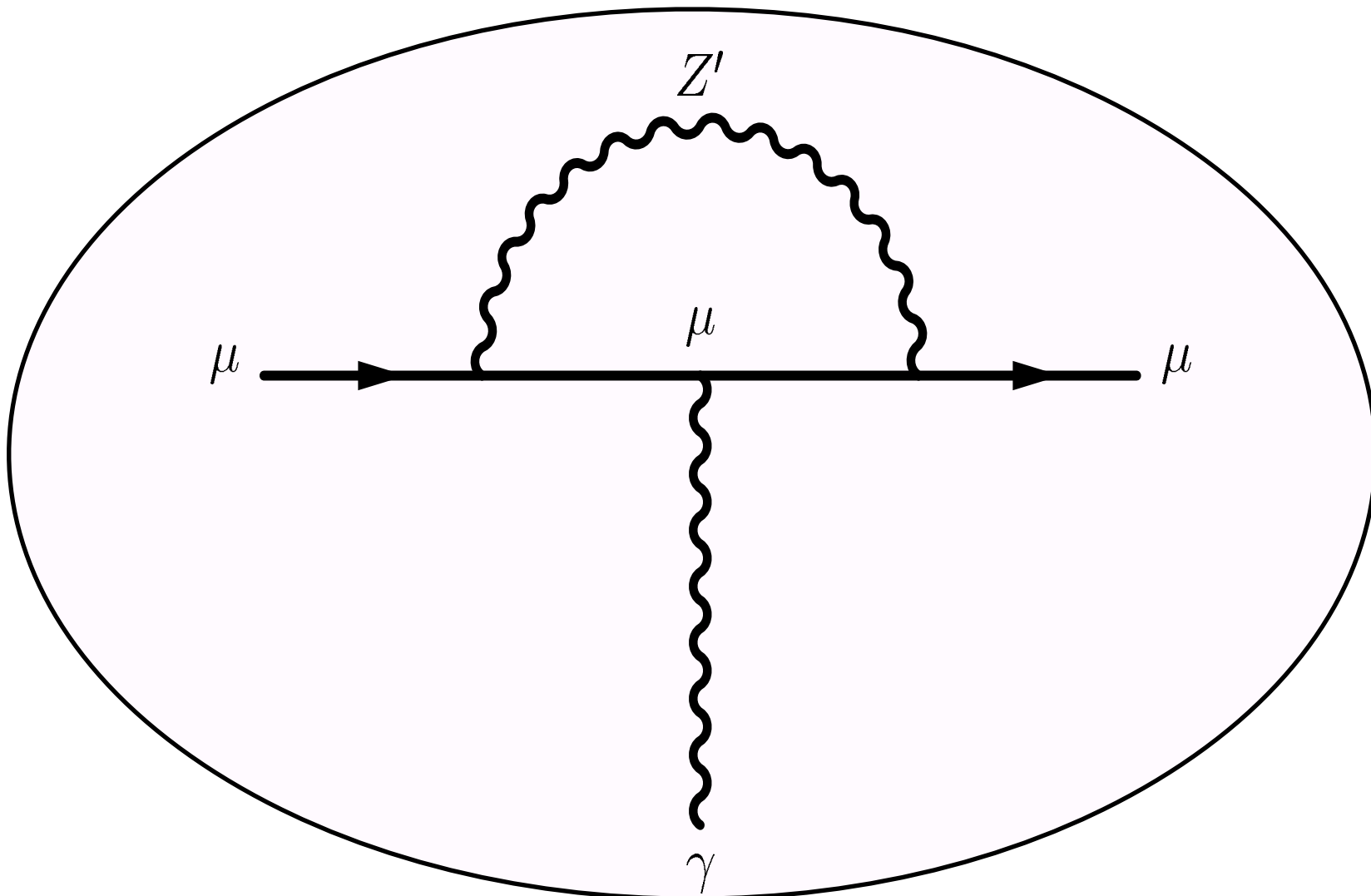


FIG. 2. Δa_μ on the a vs. $m_{Z'}$ plane in case b). The lines from left to right are for Δa_μ away from its central value at $+2\sigma, +1\sigma, 0, -1\sigma$ and -2σ , respectively.

Muon (g-2)

$$\Delta a_\mu = a_\mu^{\text{exp}} - a_\mu^{\text{SM}} = (302 \pm 88) \times 10^{-11}.$$



$$\Delta a_\mu = \frac{\alpha'}{2\pi} \int_0^1 dx \frac{2m_\mu^2 x^2(1-x)}{x^2 m_\mu^2 + (1-x)M_{Z'}^2} \approx \frac{\alpha'}{2\pi} \frac{2m_\mu^2}{3M_{Z'}^2}$$

Baek and Ko, arXiv:0811.1646, for PAMELA e^+ excess

$$\mathcal{L}_{\text{Model}} = \mathcal{L}_{\text{SM}} + \mathcal{L}_{\text{New}}$$

$$\begin{aligned}\mathcal{L}_{\text{New}} = & -\frac{1}{4}Z'_{\mu\nu}Z'^{\mu\nu} + \overline{\psi_D}iD \cdot \gamma\psi_D - M_{\psi_D}\overline{\psi_D}\psi_D + D_\mu\phi^*D^\mu\phi \\ & -\lambda_\phi(\phi^*\phi)^2 - \mu_\phi^2\phi^*\phi - \lambda_{H\phi}\phi^*\phi H^\dagger H.\end{aligned}$$

Here we ignored kinetic mixing for simplicity

$$D_\mu = \partial_\mu + ieQA_\mu + i\frac{e}{s_Wc_S}(I_3 - s_W^2Q)Z_\mu + ig'Y'Z'_\mu$$

We will study the following observables:
Muon g-2, Leptophilic DM, Collider Signature

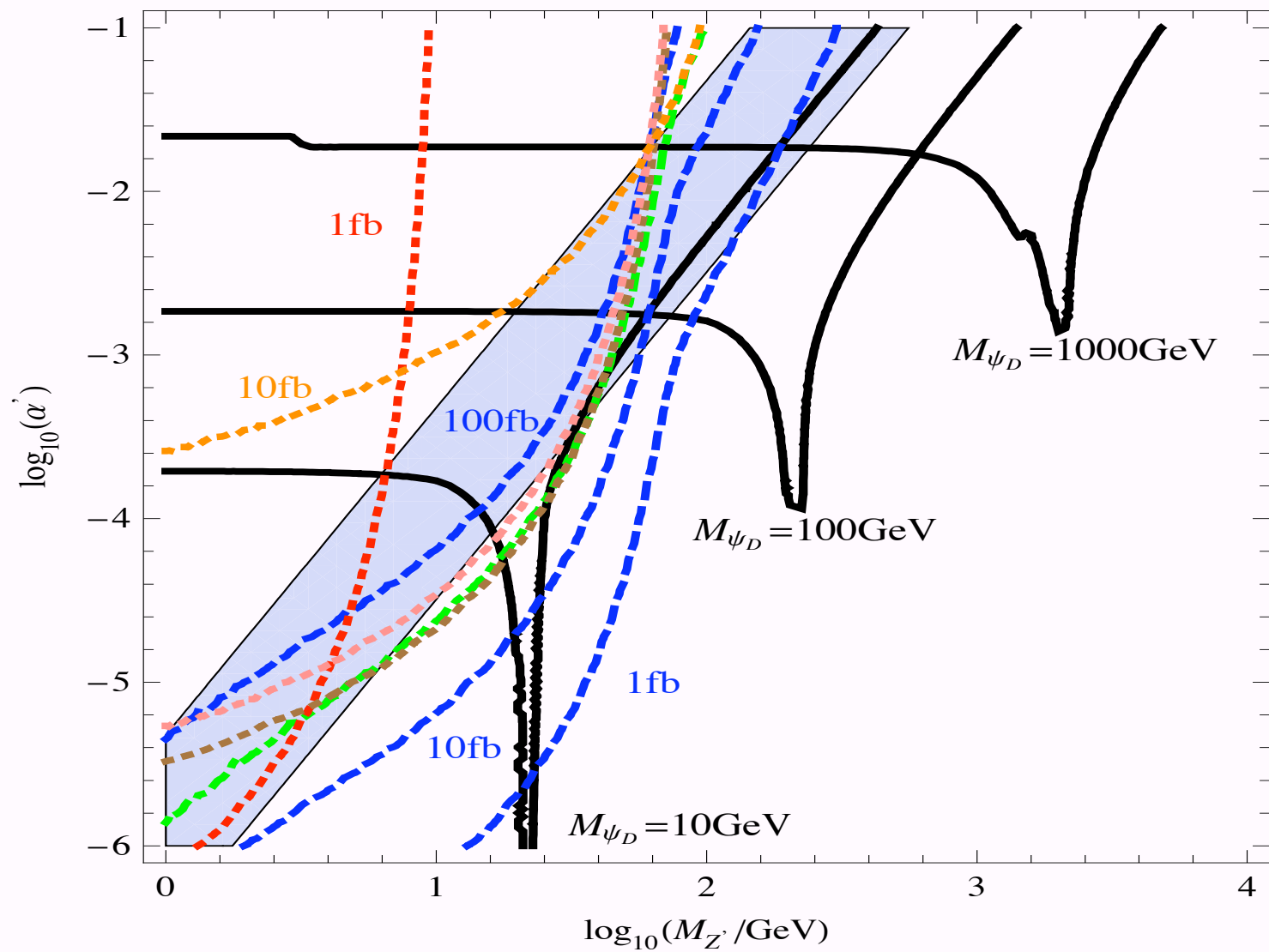


Figure 1: The relic density of CDM (black), the muon $(g - 2)_\mu$ (blue band), the production cross section at B factories (1 fb, red dotted), Tevatron (10 fb, green dotdashed), LEP (10 fb, pink dotted), LEP2 (10 fb, orange dotted), LHC (1 fb, 10 fb, 100 fb, blue dashed) and the Z^0 decay width (2.5×10^{-6} GeV, brown dotted) in the $(\log_{10} \alpha', \log_{10} M_{Z'})$ plane. For the relic density, we show three contours with $\Omega h^2 = 0.106$ for $M_{\psi_D} = 10$ GeV, 100 GeV and 1000 GeV. The blue band is allowed by $\Delta a_\mu = (302 \pm 88) \times 10^{-11}$ within 3σ .

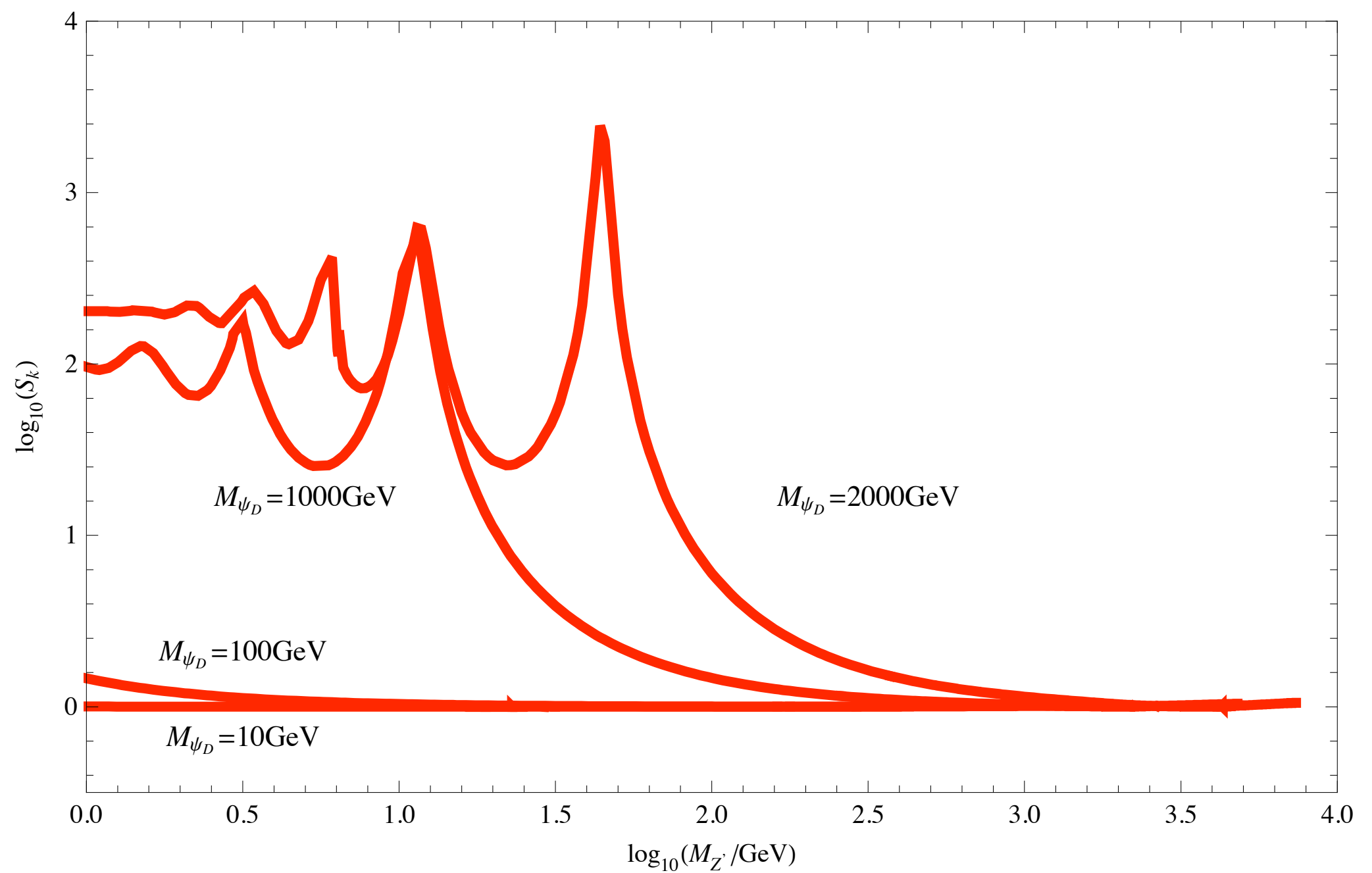
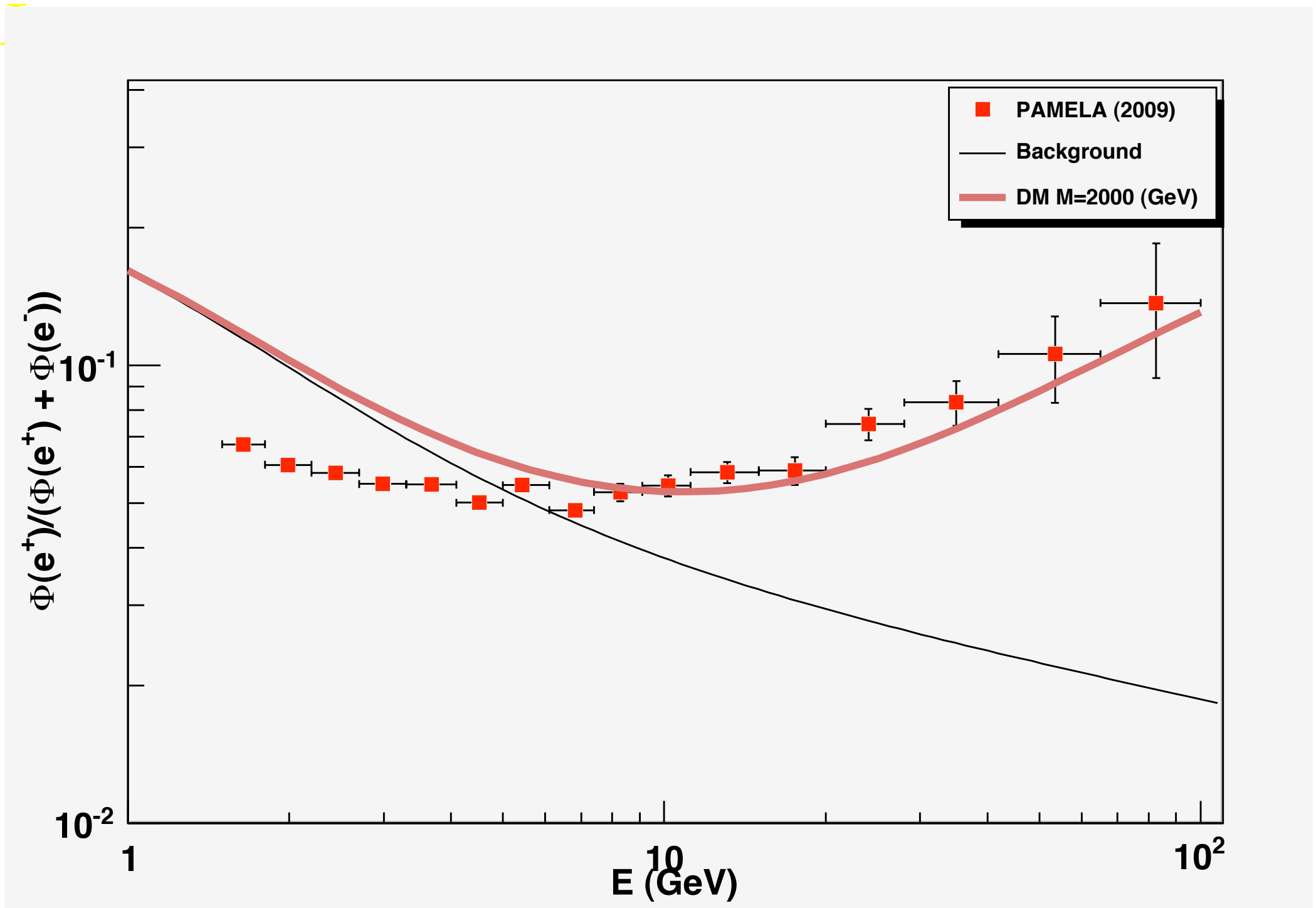
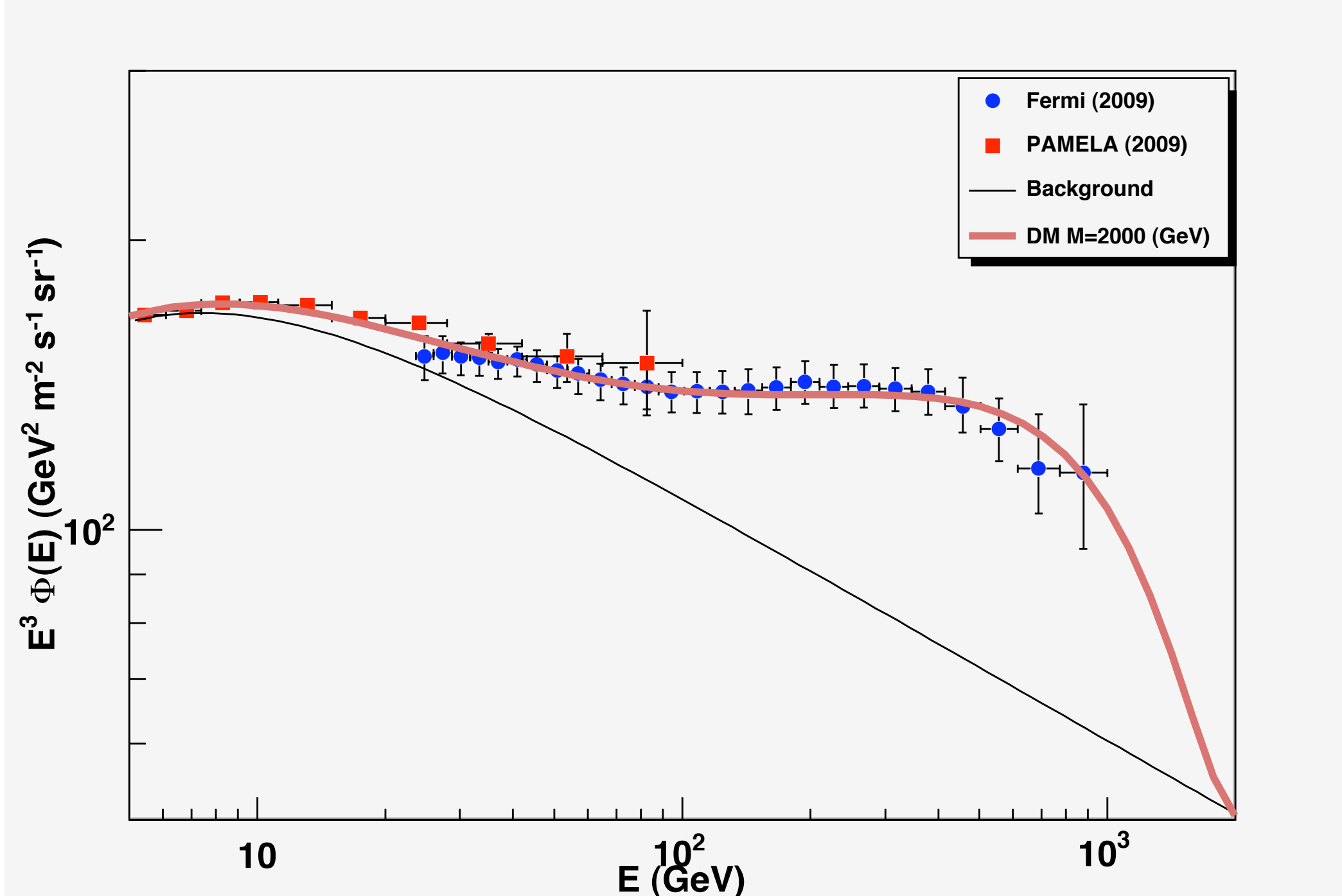


Figure: Sommerfeld enhancement factor along the constant relic density lines. $v = 200 \text{ km/s}$.

$L_\mu =$



PAMELA data on $\Phi(e^+)/(\Phi(e^-) + \Phi(e^+))$



PAMELA + FERMI with bkgd $\times 0.67$ and large
boost factor $\sim \mathcal{O}(5000)$

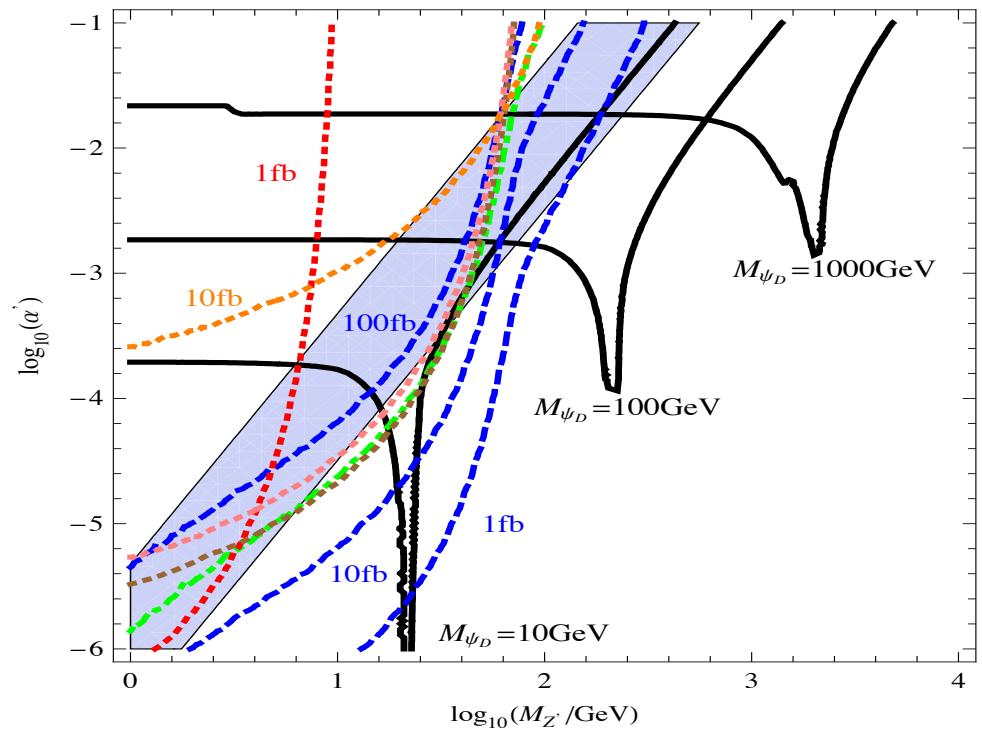


Figure 1: The relic density of CDM (black), the muon $(g - 2)_\mu$ (blue band), the production cross section at B factories (1 fb, red dotted), Tevatron (10 fb, green dotdashed), LEP (10 fb, pink dotted), LEP2 (10 fb, orange dotted), LHC (1 fb, 10 fb, 100 fb, blue dashed) and the Z^0 decay width (2.5×10^{-6} GeV, brown dotted) in the $(\log_{10} \alpha', \log_{10} M_{Z'})$ plane. For the relic density, we show three contours with $\Omega h^2 = 0.106$ for $M_{\psi_D} = 10$ GeV, 100 GeV and 1000 GeV. The blue band is allowed by $\Delta a_\mu = (302 \pm 88) \times 10^{-11}$ within 3σ .

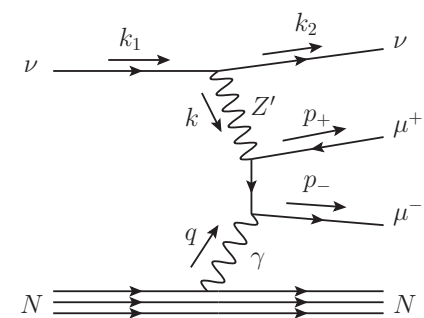


FIG. 1. The leading order contribution of the Z' to neutrino trident production (another diagram with μ^+ and μ^- reversed in g'

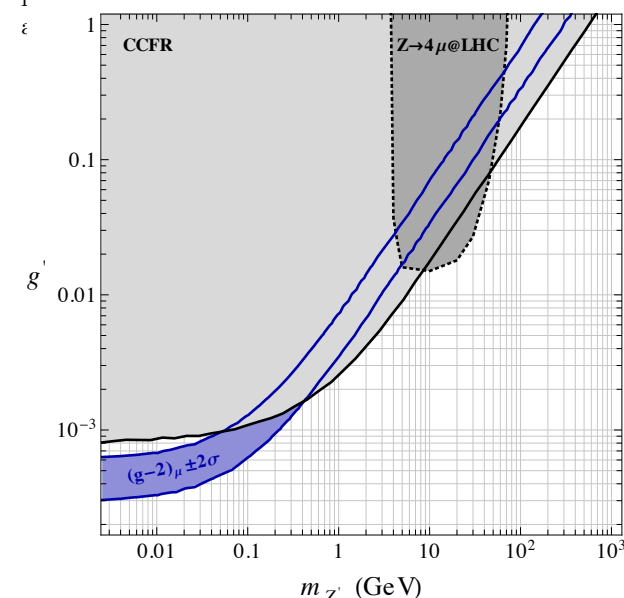


FIG. 2. Parameter space for the Z' gauge boson. The light-grey area is excluded at 95% C.L. by the CCFR measurement of the neutrino trident cross-section. The grey region with the dotted contour is excluded by measurements of the SM

**Seungwon Baek, Pyungwon Ko,
arXiv:0811.1646, JCAP(2009)
about PAMELA e^+ excess**

**Altmannshofer et al.
arXiv:1406.2332 [hep-ph]**
**Neutrino trident puts strong
constraints on this model**

**One can evade the neutrino trident constraint, if one introduces
New fermions and generate muon g-2 at loop level w/ new fermions !**

$U(1)_{L_\mu - L_\tau}$ -charged DM

: Z' only vs. $Z' + \phi$

cf: Let me call Z' , $U(1)_{L_\mu - L_\tau}$ gauge boson,
“dark photon”, since it couples to DM

Z' Only

- Consider light Z' and $g_X \sim (\text{a few}) \times 10^{-4}$ for the muon g-2. Then
- $\chi\bar{\chi} \rightarrow Z'^* \rightarrow f_{\text{SM}}\bar{f}_{\text{SM}}$: dominant annihilation channel
- $g_X \sim 10^{-4}$ is too small for $\chi\bar{\chi} \rightarrow Z'Z'$ to be effective for $\Omega_\chi h^2$
- $m_{Z'} \sim 2m_{\text{DM}}$ with the s-channel Z' resonance for the correct relic density (both for Dirac and complex scalar DM)
- Many recent studies on this case:

- Asai, Okawa, Tsumura, 2011.03165
- Holst, Hooper, Krnjaic, 2107.09067
- Drees and Zhao, arXiv:2107.14528
- And some earlier papers

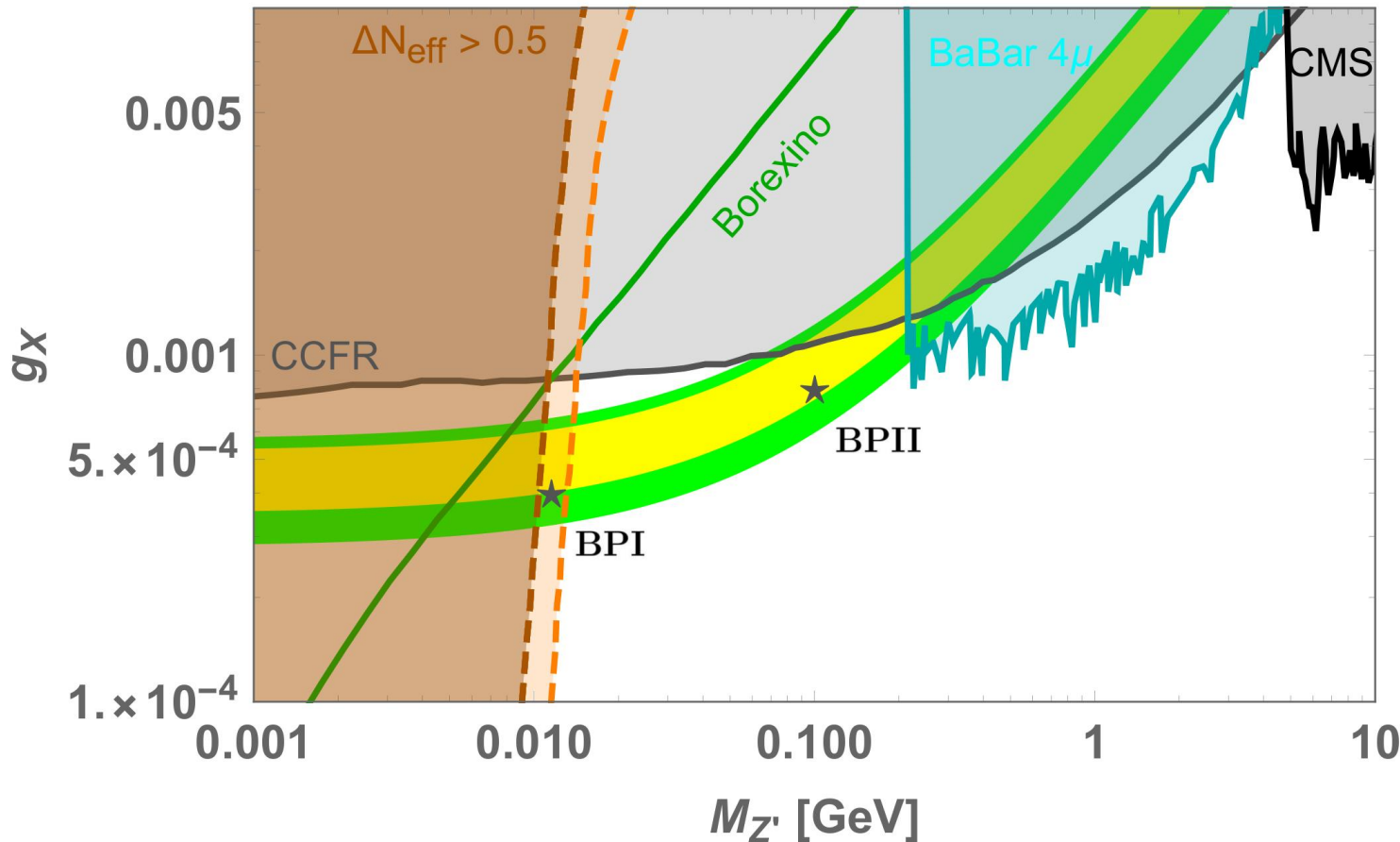


FIG. 1. Regions inside the yellow and Green shaded areas by the Δa_μ are allowed at 1σ and 2σ C.L.. Cyan, black, and orange regions are excluded by other experimental bounds. Above green solid line is ruled out by the Borexino experiment. Region inside the orange area can resolve the Hubble tension. We take two Benchmark Points (BP) ($M_{Z'}$, g_X) as **BPI** = (11.5 MeV, 4×10^{-4}) and **BPII** = (100 MeV, 8×10^{-4}).

Models with Φ

TABLE I: $U(1)$ charge assignments of newly introduced particles and SM particles. The other SM particles are singlet.

Field	Z'_μ	$X(\chi)$	Φ	$L_\mu = (\nu_{L\mu}, \mu_L), \mu_R$	$L_\tau = (\nu_{L\tau}, \tau_L), \tau_R$
spin	1	0 (1/2)	0	1/2	1/2
$U(1)$ charge	0	$Q_X(Q_\chi)$	Q_Φ	+1	-1

We consider both complex scalar (X) and Dirac fermion DM (χ)

- Physics crucially depends on Q_Φ , Q_X and Q_χ
- $Q_\Phi = 2Q_{X(\chi)}$ and $3Q_X$ need special cares, since there are extra gauge invariant op's that break $U(1) \rightarrow Z_2$, Z_3 after $U(1)$ is spontaneously broken by nonzero VEV of Φ

Complex Scalar DM (generic with $\mathcal{Q}_\Phi \neq \mathcal{Q}_X$, etc)

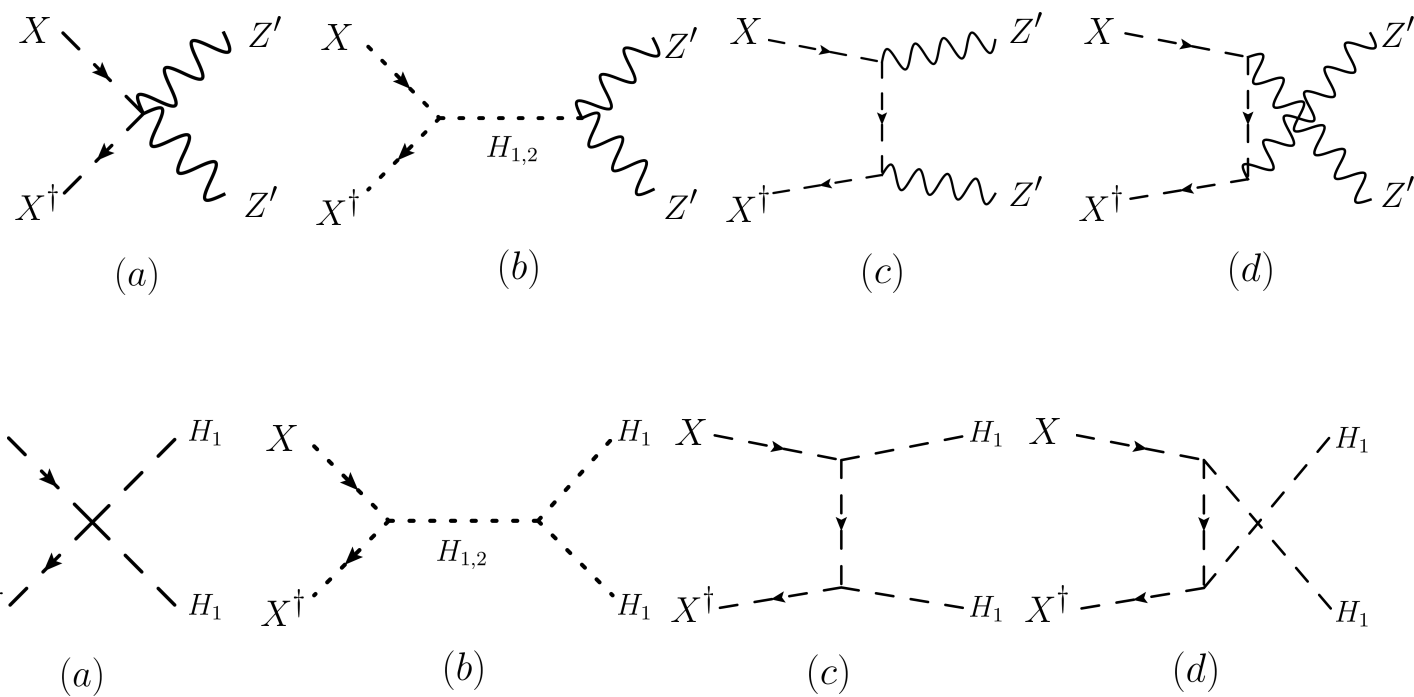


FIG. 2. (Top) Feynman diagrams for Complex scalar DM annihilating to a pair of Z' bosons. (Bottom) Feynman diagrams for Complex scalar DM annihilating to a pair of H_1 bosons.

$H_2 \simeq H_{125}$ and $H_1 \simeq \phi$ (dark Higgs)

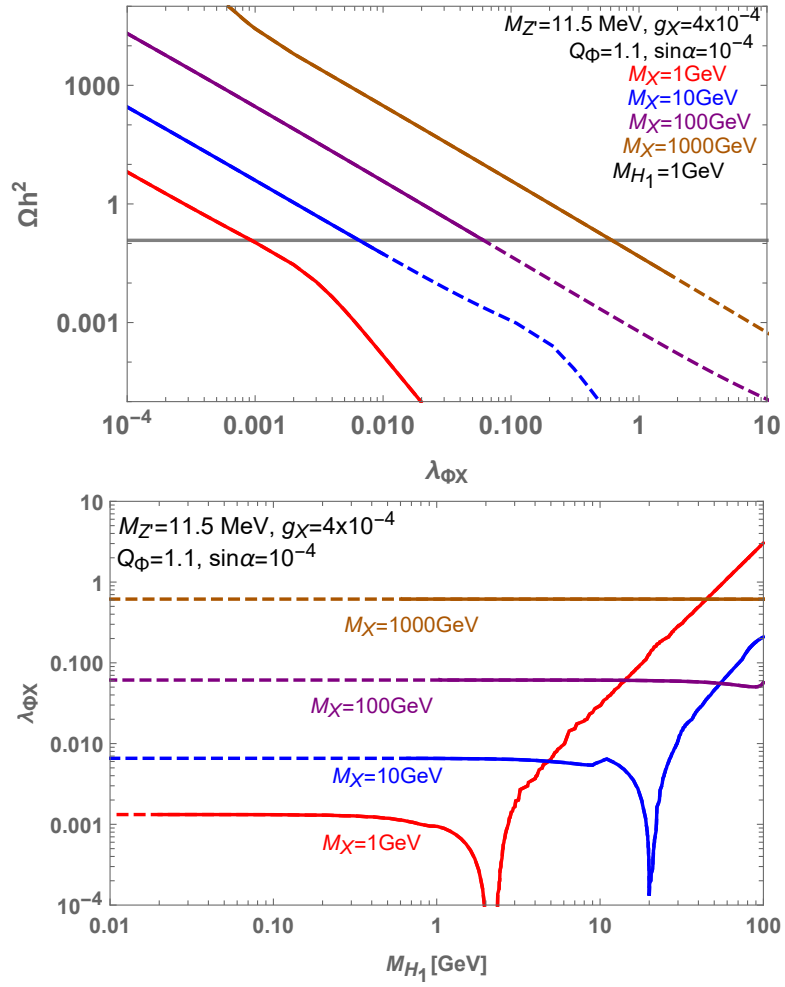


FIG. 3. *Top*: relic abundance of complex scalar DM as functions of $\lambda_{\Phi X}$ for [BPI] for $M_X = 1, 10, 100, 1000 \text{ GeV}$, respectively. We assumed $Q_\Phi = 1.1$, $M_{H_1} = 1 \text{ GeV}$, and $\sin \alpha = 10^{-4}$. Solid (Dashed) lines represent the region where bounds on DM direct detection are satisfied (ruled out). *Bottom*: the preferred parameter space in the $(M_{H_1}, \lambda_{\Phi X})$ plane for $\lambda_{HX} = 0$.

**DM mass : much wider range than $m_{Z'} \sim 2m_{\text{DM}}$
due to dark Higgs boson contributions**

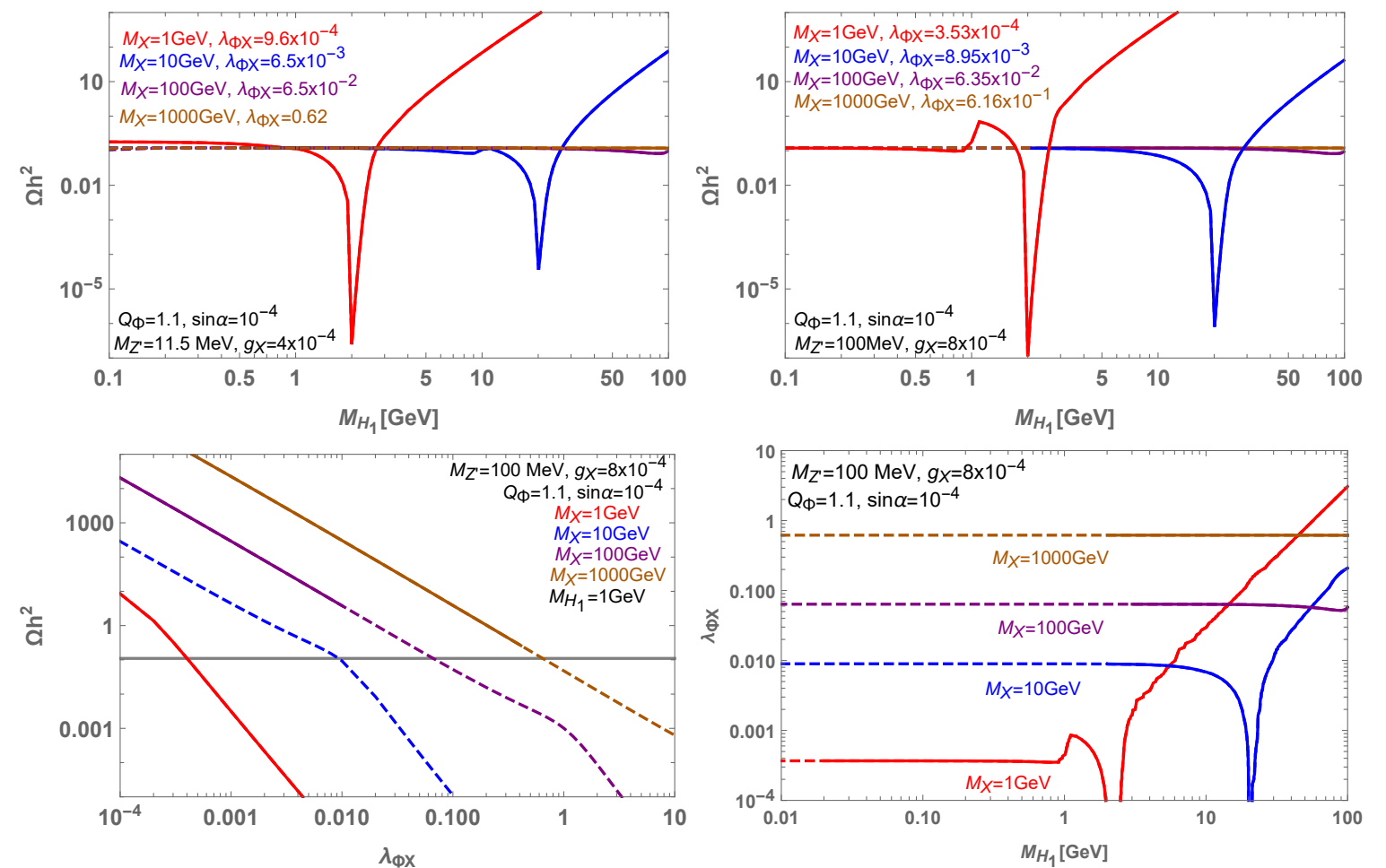


FIG. 7. The (*Top*) plots show the relic abundance of complex scalar DM for $Q_\Phi = 1.1$ as functions of dark Higgs mass M_{H_1} for [BPI] (*Left*) and [BPII] (*Right*). The (*Bottom*) plots show the relic density as functions of $\lambda_{\Phi X}$ (*Left*) and the preferred parameter space in the $(M_{H_1}, \lambda_{\Phi X})$ plane for $\lambda_{HX} = 0$ (*Right*) for [BPII]. We take four different DM masses, $M_X = 1, 10, 100, 1000 \text{ GeV}$, respectively. Solid (Dashed) lines represent the region where bounds on DM direct detection are satisfied (ruled out).

Complex Scalar DM:

$$U(1)_{L_\mu - L_\tau} \rightarrow Z_2 \ (\mathcal{Q}_\Phi = 2\mathcal{Q}_X)$$

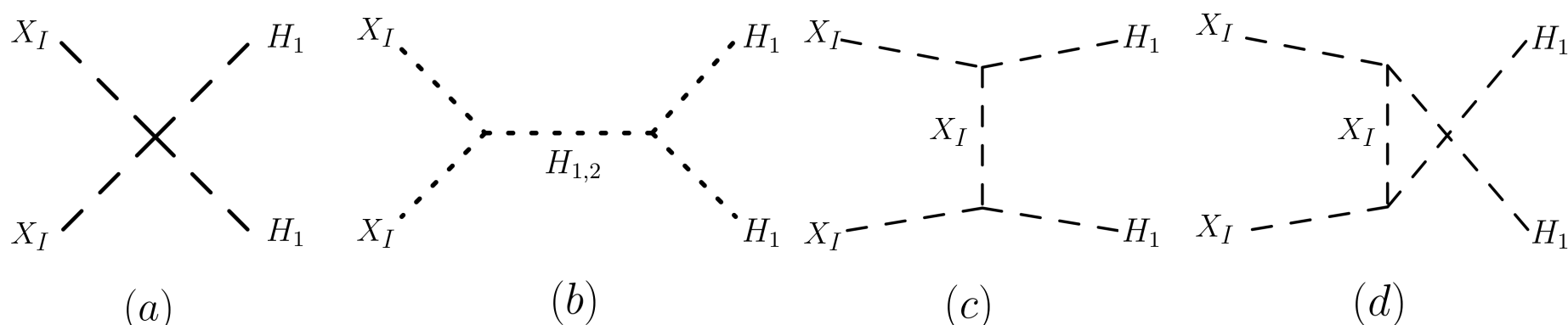
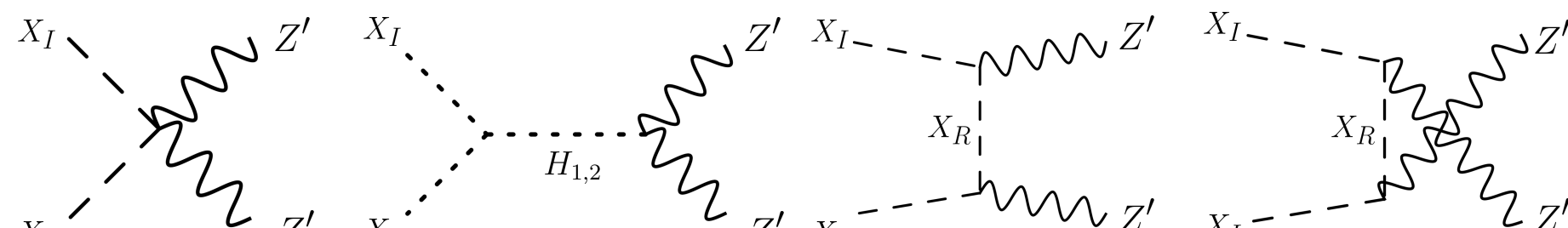


FIG. 8. (Top) Feynman diagrams for local Z_2 scalar DM annihilating to a pair of Z' bosons. (Bottom) Feynman diagrams for local Z_2 scalar DM annihilating to a pair of H_1 bosons, which is mostly dark Higgs-like.

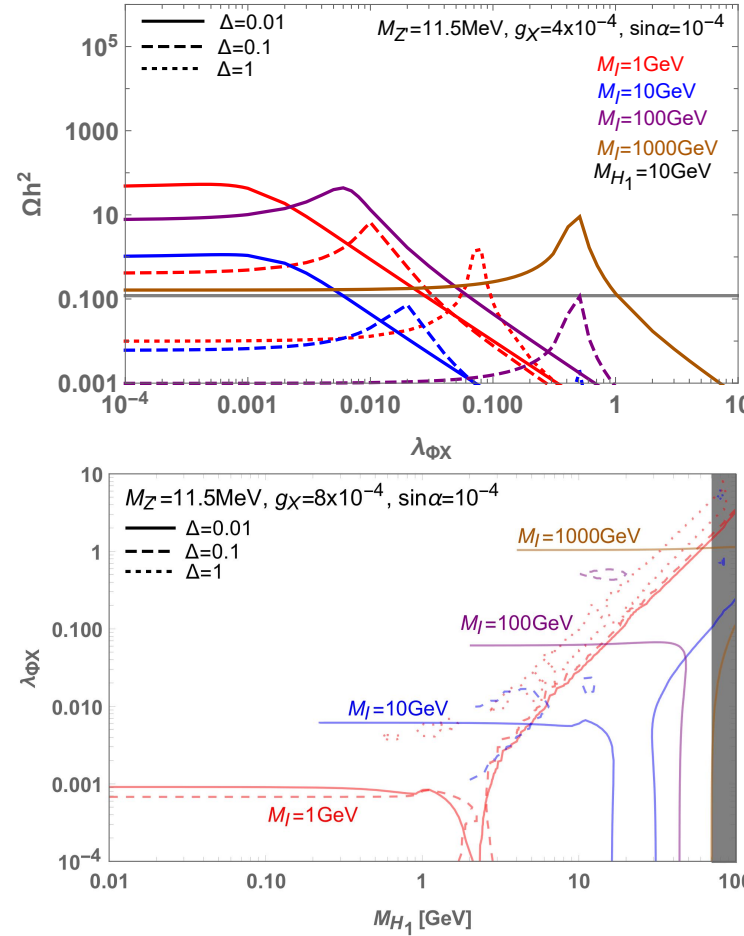


FIG. 4. *Top*: Relic abundance of local Z_2 scalar DM as functions of $\lambda_{\Phi X}$ for [BPI] and different values of mass splittings (Δ). We take $\lambda_{HX} = 0$, $M_{H_1} = 10\text{GeV}$, and $s_\alpha = 10^{-4}$. All the curves satisfy the DM direct detection bound. *Bottom*: The preferred parameter space in the $(M_{H_1}, \lambda_{\Phi X})$ plane for different values of Δ . The gray area is excluded by the perturbative condition.

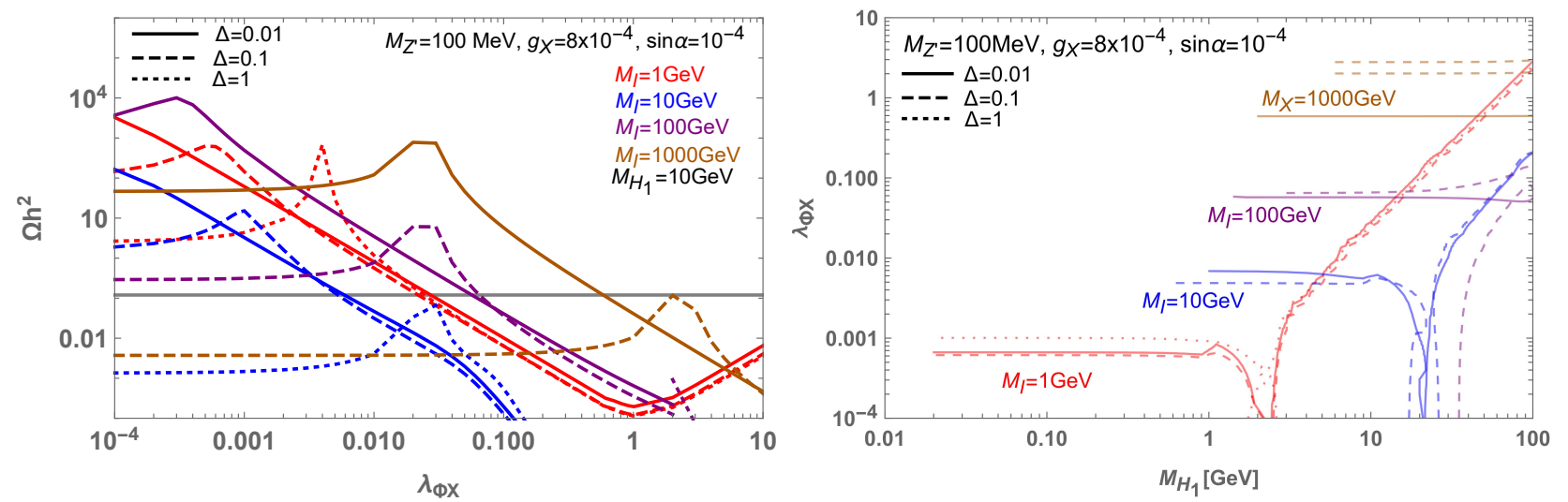


FIG. 9. (Left) Relic abundance of local Z_2 scalar DM in case of [BPII]. We take $\lambda_{HX} = 0$, $M_{H_1} = 10\text{GeV}$, and $s_\alpha = 10^{-4}$. All the lines satisfy the DM direct detection bound. (Right) Relic abundance of local Z_2 scalar DM in the $(M_{H_1}, \lambda_{\Phi X})$ plane.

DM mass : much wider range than $m_{Z'} \sim 2m_{\text{DM}}$ due to dark Higgs boson contributions

Complex Scalar DM:

$$U(1)_{L_\mu - L_\tau} \rightarrow Z_3 \quad (\mathcal{Q}_\Phi = 3\mathcal{Q}_X)$$

Local Z_3 DM Model : first considered by Ko, Tang:

arXiv:1402.6449 (SIDM), 1407.5492 (GC γ -ray excess)

$$\begin{aligned} V = & -\mu_H^2 H^\dagger H + \lambda_H (H^\dagger H)^2 - \mu_\phi^2 \phi_X^\dagger \phi_X + \lambda_\phi (\phi_X^\dagger \phi_X)^2 + \mu_X^2 X^\dagger X + \lambda_X (X^\dagger X)^2 \\ & + \lambda_{\phi H} \phi_X^\dagger \phi_X H^\dagger H + \lambda_{\phi X} X^\dagger X \phi_X^\dagger \phi_X + \lambda_{HX} X^\dagger X H^\dagger H + \left(\lambda_3 X^3 \phi_X^\dagger + H.c. \right) \end{aligned} \quad (2.1)$$

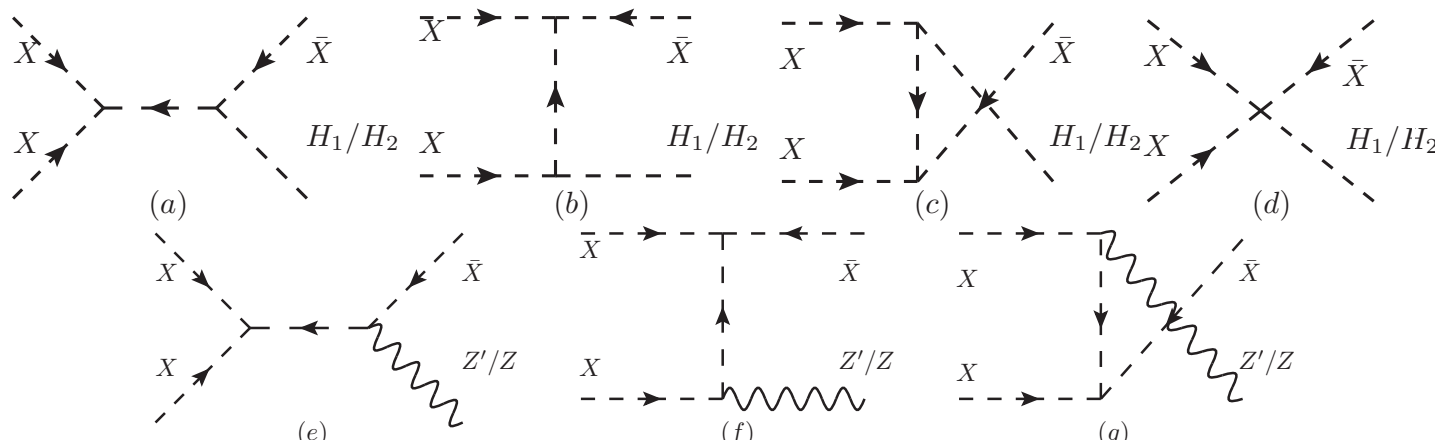
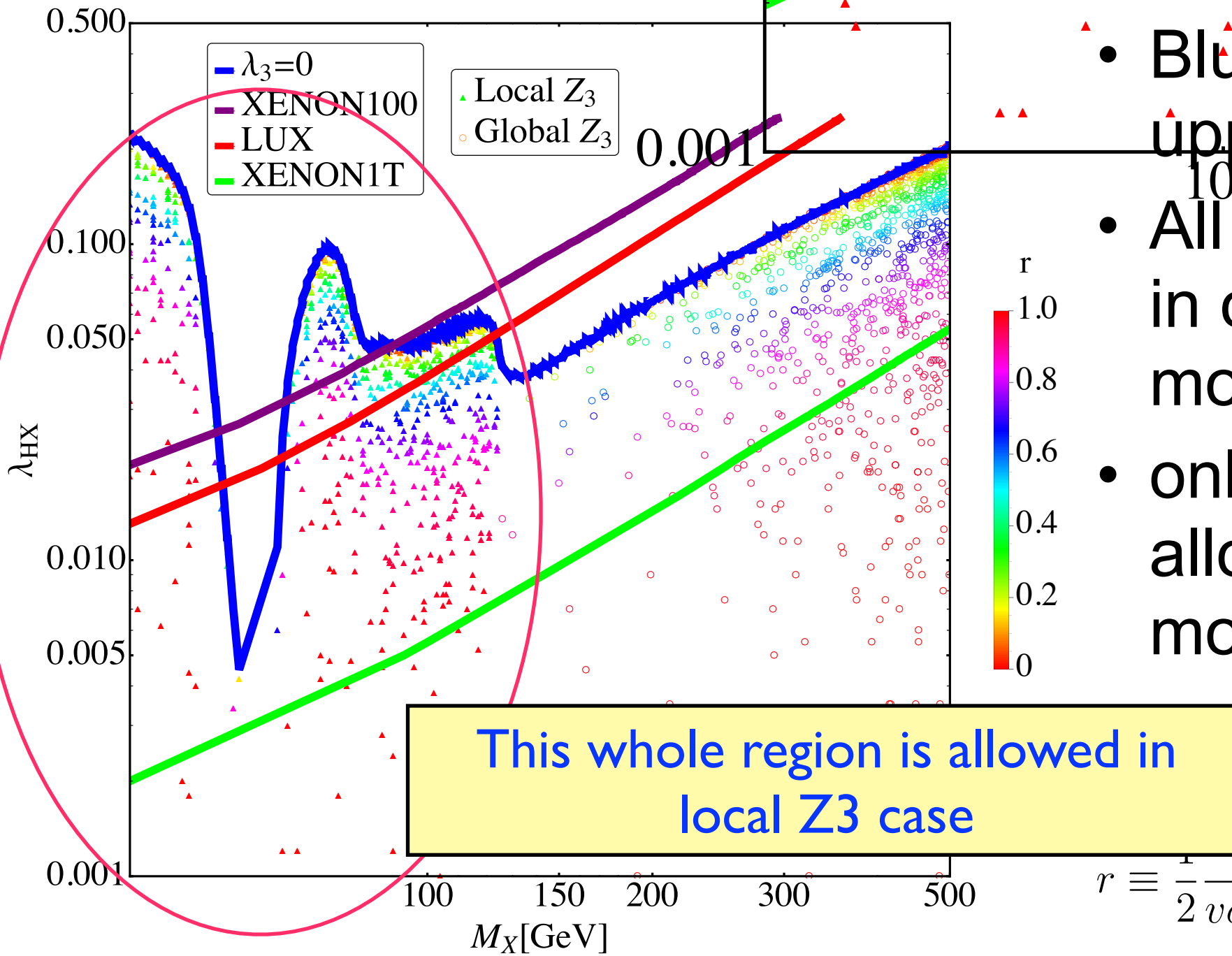


FIG. 1: Feynman diagrams for dark matter semi-annihilation. Only (a), (b), and (c) with H_1 as final state appear in the global Z_3 model, while all diagrams could contribute in local Z_3 model.

**ϕ and Z' : present only in models with dark gauge symmetries,
And not in models with global dark symmetries**

Dark $U(1) \rightarrow Z_3$

$$\Omega h^2 \subset [0.1145, 0.1253], \lambda_3 < 0.02$$



- Blue band marks the upper bound,
- All points are allowed in our local Z_3 model, 1402.6449
- only circles are allowed in global Z_3 model, 1211.1014

$$r \equiv \frac{v\sigma^{XX \rightarrow X^*Y}}{\frac{1}{2}v\sigma^{XX^* \rightarrow YY} + \frac{1}{2}v\sigma^{XX \rightarrow X^*Y}}.$$

$U(1)_{L_\mu - L_\tau} \rightarrow Z_3$

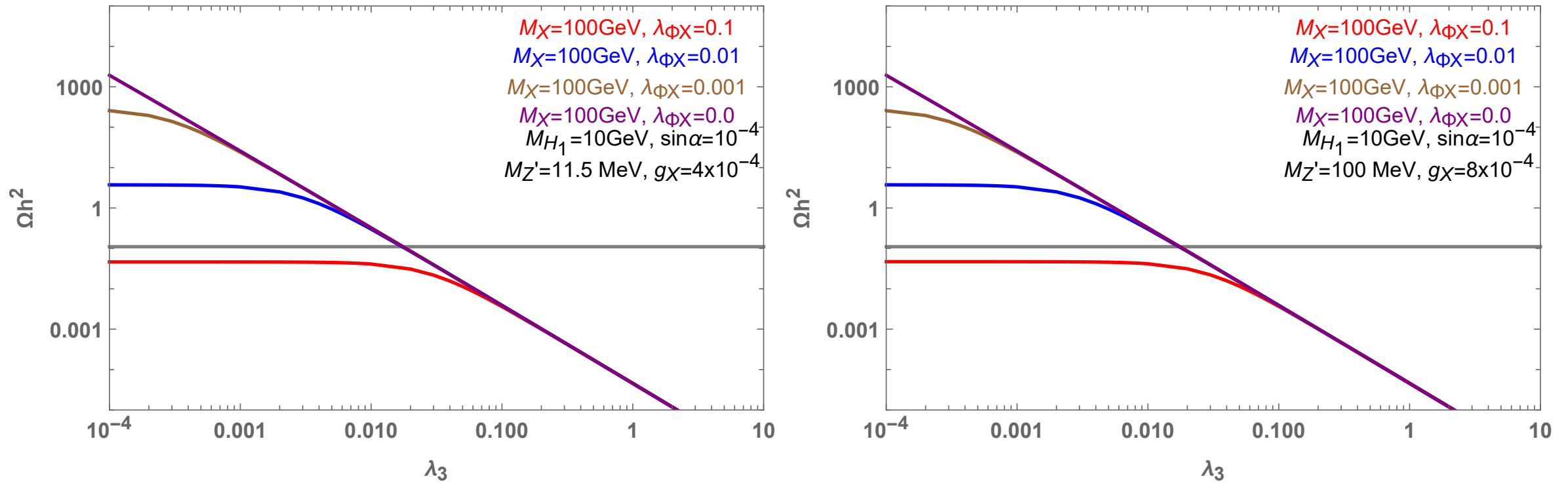


FIG. 10. Relic abundance of Z_3 scalar DM for the [BP I] (Left) and the [BP II] (Right), respectively. Here we fixed $\lambda_{HX} = 0$ for simplicity.

- $g_X \sim O(10^{-4})$: very small. $XX \rightarrow X^\dagger Z'$ is not important

DM mass : much wider range than $m_{Z'} \sim 2m_{\text{DM}}$
 due to dark Higgs boson contributions
- λ_3 controlling $XX \rightarrow X^\dagger H_1$ is an important parameter

Dirac fermion DM:

$$U(1)_{L_\mu - L_\tau} \rightarrow Z_2 \quad (Q_\Phi = 2 Q_\chi)$$

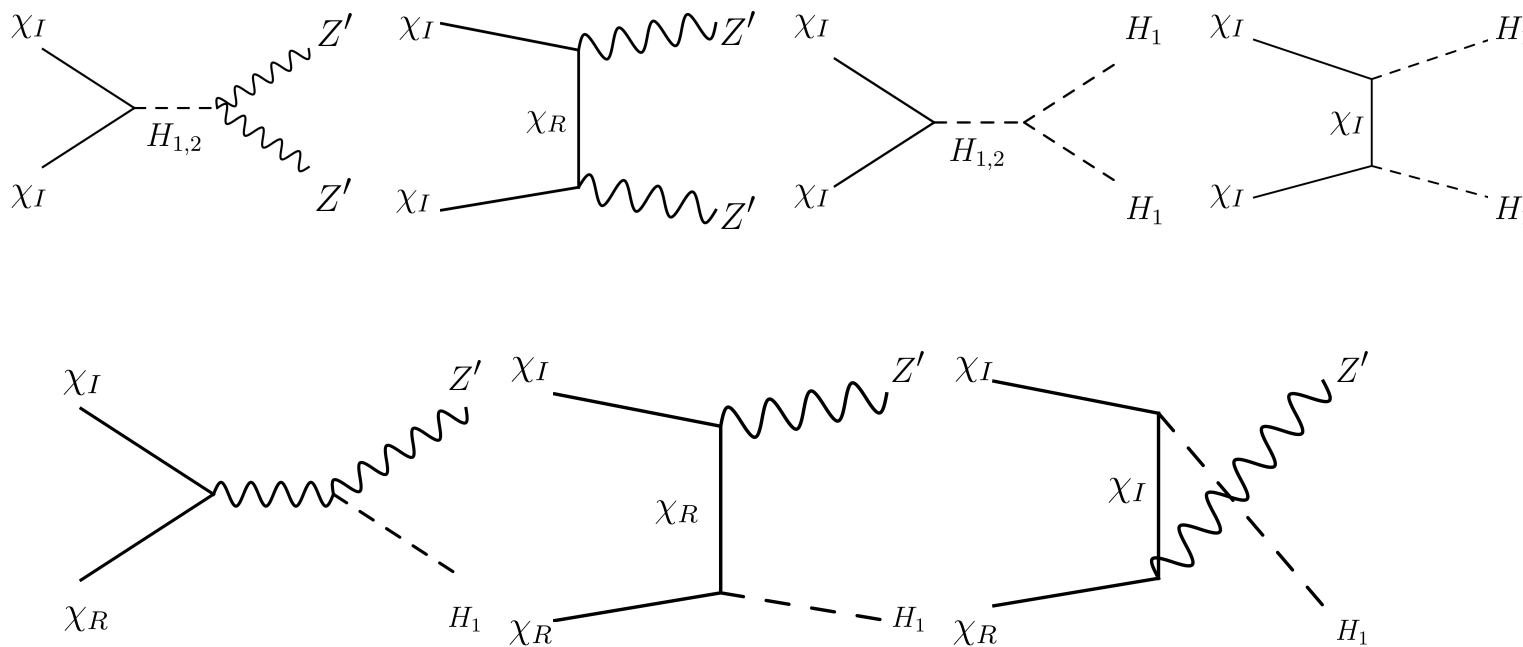


FIG. 5. Feynman diagrams of local Z_2 fermion DM (co-)annihilating into a pair of Z' bosons and H_1 bosons (*Top*), and $Z' + H_1$ (*Bottom*).

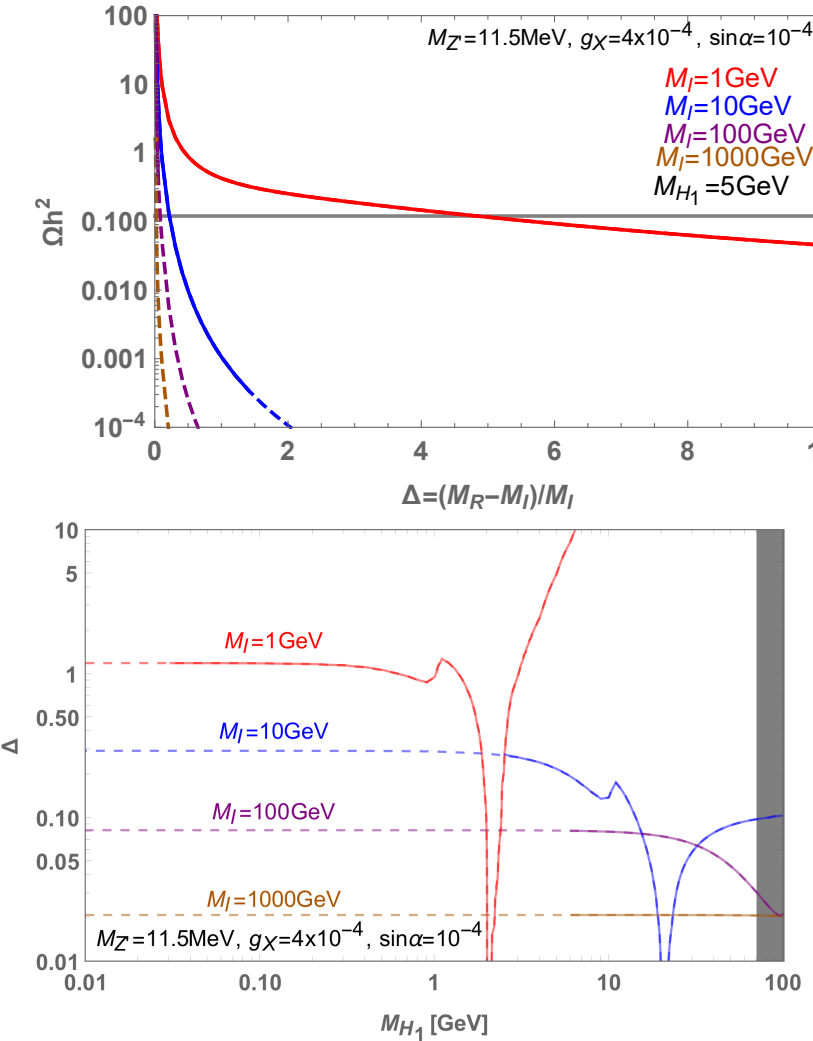


FIG. 6. *Top*: Dark matter relic density as functions of mass splitting Δ for [BPI] and for different values of DM mass, $M_I = 1, 10, 100, 1000 \text{ GeV}$. Solid (Dashed) lines denote the region where bounds on DM direct detection are satisfied (ruled out). *Bottom*: Preferred parameter space in the (M_{H_1}, Δ) plane for different DM masses. The gray region is ruled out by the perturbativity condition on λ_Φ .

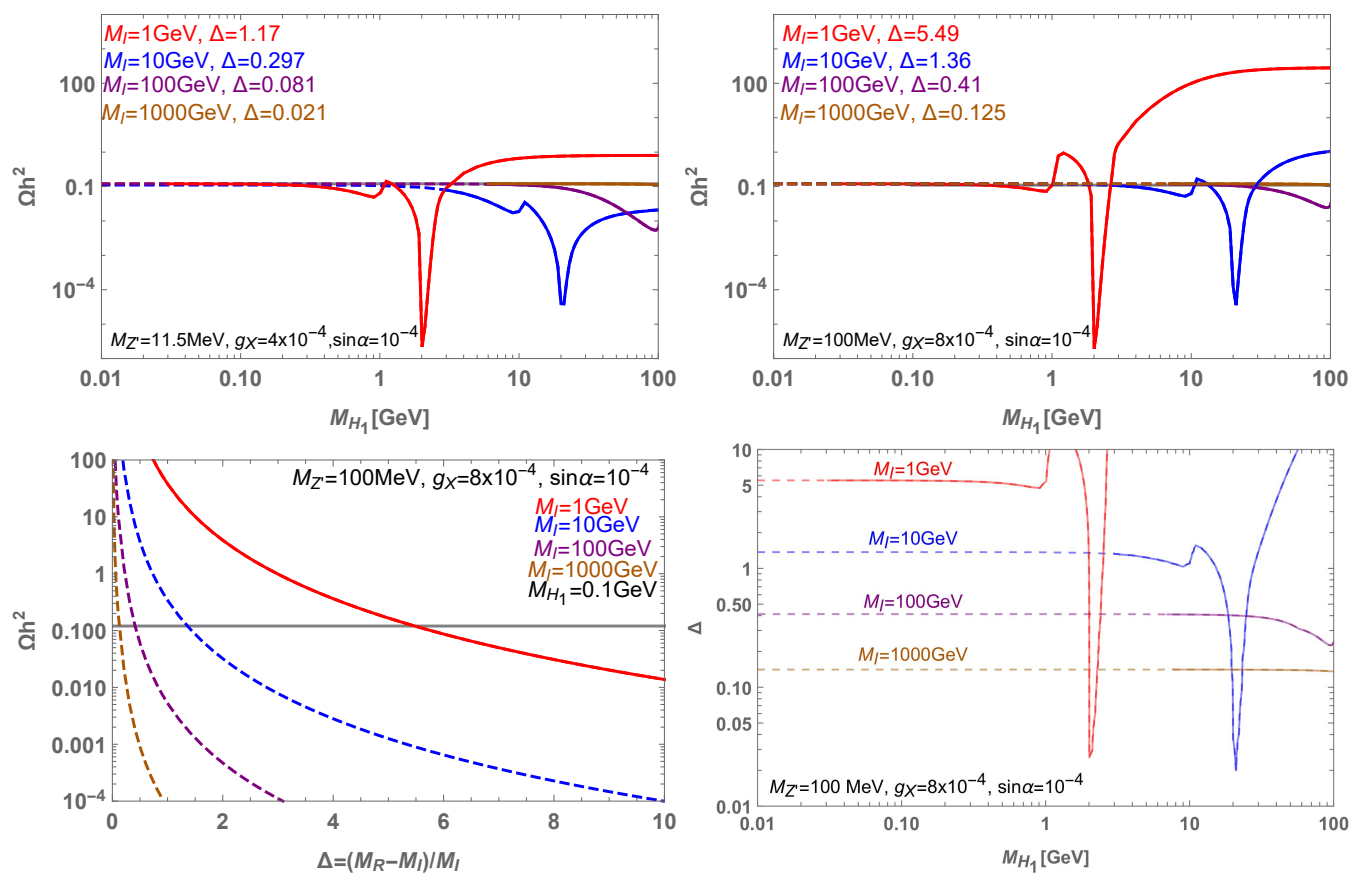


FIG. 11. *(Top)* Dark matter relic density as functions of dark Higgs mass M_{H_1} for [BPI] (*Left*) and [BPII] (*Right*) *(Bottom-Left)* Dark matter relic density as functions of Δ for [BPII], and *(Bottom-right)* Preferred parameter region in the (Δ, M_{H_1}) plane. Solid (Dashed) lines denote the region where bounds on DM direct detection are satisfied (ruled out).

DM mass : much wider range than $m_{Z'} \sim 2m_{\text{DM}}$ due to dark Higgs boson contributions

Conclusion

- DM physics with massive dark photon can not be complete without including dark gauge symmetry breaking mechanism, e.g. dark Higgs field ϕ (or some ways other than dark Higgs to provide dark photon mass) which have been largely ignored
- Many examples show the importance of ϕ in DM phenomenology, both in (astro)particle physics and cosmology
- Once ϕ is included, can accommodate the muon g-2 and thermal DM without the s-channel resonance condition $m_{Z'} \sim 2m_{\text{DM}}$
- m_{DM} : essentially free, whereas $m_{Z'} \sim O(10 - 100)$ MeV and $g_X \sim O(10^{-4})$ can explain the muon $(g - 2)_\mu$